



Article

# Impact of Exosomes Released by Different Corneal Cell Types on the Wound Healing Properties of Human Corneal Epithelial Cells

Pascale Desjardins <sup>1,2,3,4,5</sup>, Rébecca Berthiaume <sup>1,2,3,4</sup>, Camille Couture <sup>1,2,3,4,5</sup>, Gaétan Le-Bel <sup>1,2,3,4,5</sup> , Vincent Roy <sup>1,3,5</sup>, François Gros-Louis <sup>1,3,5</sup>, Véronique J. Moulin <sup>1,3,5</sup>, Stéphanie Proulx <sup>1,2,3,4</sup> , Sylvain Chemtob <sup>6</sup>, Lucie Germain <sup>1,3,5</sup> and Sylvain L. Guérin <sup>1,2,3,4,\*</sup>

<sup>1</sup> Regenerative Medicine Division of the Centre de Recherche du CHU de Québec, Université Laval, Québec, QC G1J 1Z4, Canada

<sup>2</sup> Centre Universitaire d'Ophtalmologie (CUO)-Recherche, Hôpital du Saint-Sacrement, 1050 Chemin Ste-Foy, Québec, QC G1J 1Z4, Canada

<sup>3</sup> Centre de Recherche en Organogénèse Expérimentale de l'Université Laval/LOEX, Hôpital Enfant-Jésus, 1401 18e Rue, Québec, QC G1V 0A6, Canada

<sup>4</sup> Département d'Ophtalmologie, Faculté de Médecine, Université Laval, Québec, QC G1V 0A6, Canada

<sup>5</sup> Département de Chirurgie, Faculté de Médecine, Université Laval, Québec, QC G1V 0A6, Canada

<sup>6</sup> Département d'Ophtalmologie, Faculté de Médecine, Université de Montréal, Montréal, QC H3T 1J4, Canada

\* Correspondence: sylvain.guerin@fmed.ulaval.ca



**Citation:** Desjardins, P.; Berthiaume, R.; Couture, C.; Le-Bel, G.; Roy, V.; Gros-Louis, F.; Moulin, V.J.; Proulx, S.; Chemtob, S.; Germain, L.; et al. Impact of Exosomes Released by Different Corneal Cell Types on the Wound Healing Properties of Human Corneal Epithelial Cells. *Int. J. Mol. Sci.* **2022**, *23*, 12201. <https://doi.org/10.3390/ijms232012201>

Academic Editors: Elia Ranzato and Simona Martinotti

Received: 21 September 2022

Accepted: 6 October 2022

Published: 13 October 2022

**Publisher's Note:** MDPI stays neutral with regard to jurisdictional claims in published maps and institutional affiliations.



**Copyright:** © 2022 by the authors. Licensee MDPI, Basel, Switzerland. This article is an open access article distributed under the terms and conditions of the Creative Commons Attribution (CC BY) license (<https://creativecommons.org/licenses/by/4.0/>).

**Abstract:** Corneal wound healing involves communication between the different cell types that constitute the three cellular layers of the cornea (epithelium, stroma and endothelium), a process ensured in part by a category of extracellular vesicles called exosomes. In the present study, we isolated exosomes released by primary cultured human corneal epithelial cells (hCECs), corneal fibroblasts (hCFs) and corneal endothelial cells (hCEnCs) and determined whether they have wound healing characteristics of their own and to which point they modify the genetic and proteomic pattern of these cell types. Exosomes released by all three cell types significantly accelerated wound closure of scratch-wounded hCECs *in vitro* compared to controls (without exosomes). Profiling of activated kinases revealed that exosomes from human corneal cells caused the activation of signal transduction mediators that belong to the HSP27, STAT, β-catenin, GSK-3β and p38 pathways. Most of all, data from gene profiling analyses indicated that exosomes, irrespective of their cellular origin, alter a restricted subset of genes that are completely different between each targeted cell type (hCECs, hCFs, hCEnCs). Analysis of the genes specifically differentially regulated for a given cell-type in the microarray data using the Ingenuity Pathway Analysis (IPA) software revealed that the mean gene expression profile of hCECs cultured in the presence of exosomes would likely promote cell proliferation and migration whereas it would reduce differentiation when compared to control cells. Collectively, our findings represent a conceptual advance in understanding the mechanisms of corneal wound repair that may ultimately open new avenues for the development of novel therapeutic approaches to improve closure of corneal wounds.

**Keywords:** cornea; wound healing; exosomes; extracellular vesicles; corneal epithelial cells; corneal stromal fibroblasts; corneal endothelial cells; signal transduction pathway

## 1. Introduction

The eye is a fascinating, yet complex organ composed of many structures that allows us to see our surrounding. One such structure is the cornea, a particularly important tissue as its structural integrity is crucial for proper light transmission to the retina. In fact, corneal transparency is critical to ensure a proper visual acuity. However, because of its anterior position at the surface of the eye, the cornea is subjected to traumas such as chemical and mechanical injuries that may disturb the vision. Abrasions of the corneal

epithelium caused by fingernails [1] or sustained contact lenses wear [2] account for a large proportion of the corneal injuries. If not treated properly or rapidly, they can lead to infections, which may then progress toward more serious complications, such as ulcers and corneal perforations [3]. Moreover, traumatic events such as the propulsion of metallic debris [4,5] or chemical substances [6] in the eye can deteriorate the eye surface at a point where corneal stem cells from the limbus can no longer ensure regeneration of the corneal tissue. This can lead to corneal opacification and in more severe cases, to a complete loss of vision as a result of a syndrome known as the limbal stem cell deficiency (LSCD) [7]. In every case, a rapid and appropriate treatment of the injury allows a better recovery of visual acuity [8,9].

Corneal wound healing requires many biological processes such as cell proliferation, migration, adhesion, differentiation as well as extracellular matrix (ECM) remodeling [10]. One key aspect that regulates these events resides in the communication between cells present in each of the three corneal layers (epithelium, stroma and endothelium). The epithelium, the most outer layer of the cornea, consists of five to seven well-organized layers of corneal epithelial cells. The stroma is the thicker segment of the cornea. It is mainly composed of collagen types I and V organized into collagen fibrils, both components being secreted by the stromal fibroblasts. In turn, collagen fibrils are then organized into flattened lamellae, which are precisely superimposed one on another in a manner that allows light transmission to the retina [11]. A monolayer of endothelial cells lines the posterior limit of the cornea and actively regulates stromal hydration. Much evidence suggests that the cells from these three different corneal compartments communicate with each other to facilitate wound healing upon injury, especially when the basement membrane (BM) underneath the epithelium is disrupted. For example, abrasions that affect the epithelium prompt the secretion of fibronectin by epithelial cells as well as stromal fibroblasts. Such newly formed ECM then facilitates the migration of the epithelial cells to cover the wound [12]. In addition, it is known that cytokines such as TGF- $\beta$ 1 and PDGF secreted by epithelial cells can pass through the discontinued BM in order to trigger differentiation of the stromal fibroblasts into myofibroblasts, which is useful for the wounding process [13]. Moreover, these myofibroblasts produce growth factors such as HGF and KGF, which will in turn contribute to the proliferation of the corneal epithelial cells [14]. The endothelial-mesenchymal transition also represents another such example, this process being triggered by the secretion of FGF-2 by corneal epithelial cells during epithelial wound healing [15,16].

Despite the fact that there is a clear communication between the three layers of the cornea, little is known about how this communication occurs. This process undoubtedly involves extracellular vesicles (EVs), and more particularly a relatively small class of EVs called exosomes. Exosomes typically range from 30 to 150 nm of diameter and are derived from multivesicular bodies that escape the lysosomal degradation [17–19]. When released by the cell through exocytosis [20], exosomes can either act on nearby cells or travel long distances via the blood and lymphatic vessels [21,22] to reach other tissues or organs. An interesting feature of the exosomes is their capacity to carry various bioactive cargos such as lipids [23], proteins [24,25], miRNAs [26–29], long non-coding RNAs [30,31], etc. By taking part into intercellular communication, exosomes are indeed involved in maintaining biological homeostasis, as well as in a plethora of other biological and pathological processes, including inflammation, cancer progression and wound healing [32–35]. Furthermore, because they can carry various molecules, exosomes are now being tested as drug carriers to treat diseases such as Parkinson disease [36], pancreatic cancers [37] and lung diseases [38]. The use of exosomes as low-invasive biomarkers for detecting and monitoring several pathologies is also an active area of investigation [39].

Although exosomes were discovered in the early nineties [40], their study gained popularity only 30 years later. This explains why little is known about exosomes, especially in the cornea. However, it was established that corneal epithelial cells [41], stromal fibroblasts [42] and endothelial cells [43] indeed release exosomes [44]. Moreover, EVs have been

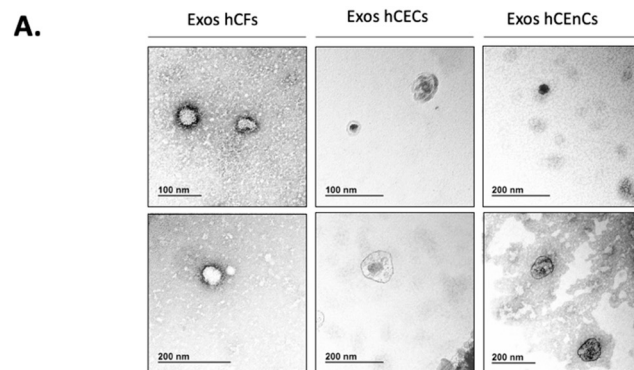
found to be secreted in the cornea following wounding [41] and it is known that exosomes secreted by corneal epithelial cells can pass through the BM if impaired by an injury [41]. These results all pointed to a potential role of exosomes in corneal wound healing, which has recently been the focus of a few studies [41,42,45–48]. However, characteristics, functional roles and mechanisms of action of corneal exosomes remain to be fully investigated. In the present study, we evaluated the capacity of exosomes released by human corneal epithelial cells (hCECs), human corneal fibroblasts (hCFs) and human corneal endothelial cells (hCEnCs) to alter the genetic and proteomic profiling of each of these cell types and determined whether they have distinctive wound healing characteristics of their own.

## 2. Results

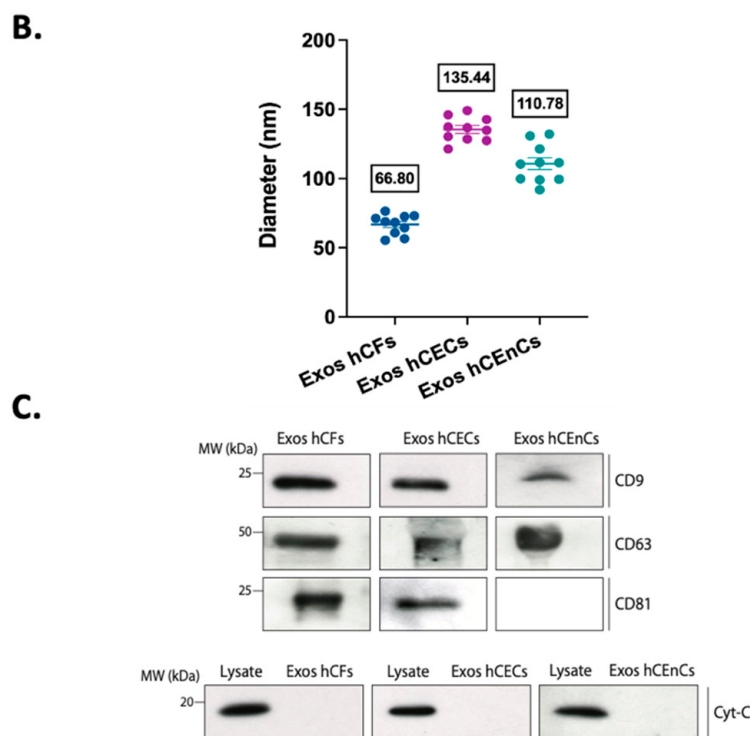
### 2.1. Characterization of the Exosomes Derived from the Three Different Corneal Cell Types

The production of exosomes has been reported to vary greatly between different cell types, especially in cells from the immune system [49]. However, and to our knowledge, no such analysis has ever been reported for the different cell types that constitute the human cornea. In order to verify the capacity of the different corneal cells to release exosomes in their surroundings, we primary cultured human corneal epithelial (hCECs), fibroblast (hCFs) and endothelial (hCEnCs) cells as monolayers. Exosomes were then enriched by ultracentrifugation from the conditioned media of these cultured cells. Figure 1A shows typical exosomes isolated from each cell population, as seen by transmission electron microscopy (TEM). Their round morphology (often with a central depression) and sizes are well-established features of such small extracellular vesicles [50]. Their size was further determined by Dynamic Light Scattering (DLS) and are shown on Figure 1B. Results indicate that exosomes' diameters vary from 67 to 135 nm between the three corneal cell types, which correspond to the typical range of sizes for exosomes as observed in the literature [51,52]. Moreover, we also assessed the presence of the exosome markers CD9, CD63 and CD81 in our samples. Western blot analyses revealed that those isolated from hCECs and hCFs were all enriched with the typical exosomes tetraspanin protein markers CD9, CD63 and CD81 [53] whereas those from hCEnCs were positive for both CD9 and CD63 but not for CD81 (Figure 1C).

It is now widely accepted that obtaining a pure sample, exclusively enriched in exosomes, is more a utopia than a tangible prospect [54]. Although probably mostly composed of exosomes, our samples also present a little heterogeneity, as revealed by high-sensitivity, flow cytometry experiments (Supplementary Figure S1). Several observations can be drawn from these analyses. First, we can see that most of the extracellular vesicles (EVs) contained in our samples present sizes ranging from 100 to 500 nm. However, a minority of them have sizes greater than 500 nm and up to 1000 nm for the densest samples. Another interesting piece of information is that different populations of extracellular vesicles, that either stain positive or negative for one or more EVs markers (AnnexinV, CD63 and CellTracker Deep Red) could be observed. This serves as a good example to illustrate heterogeneity of the EVs samples.



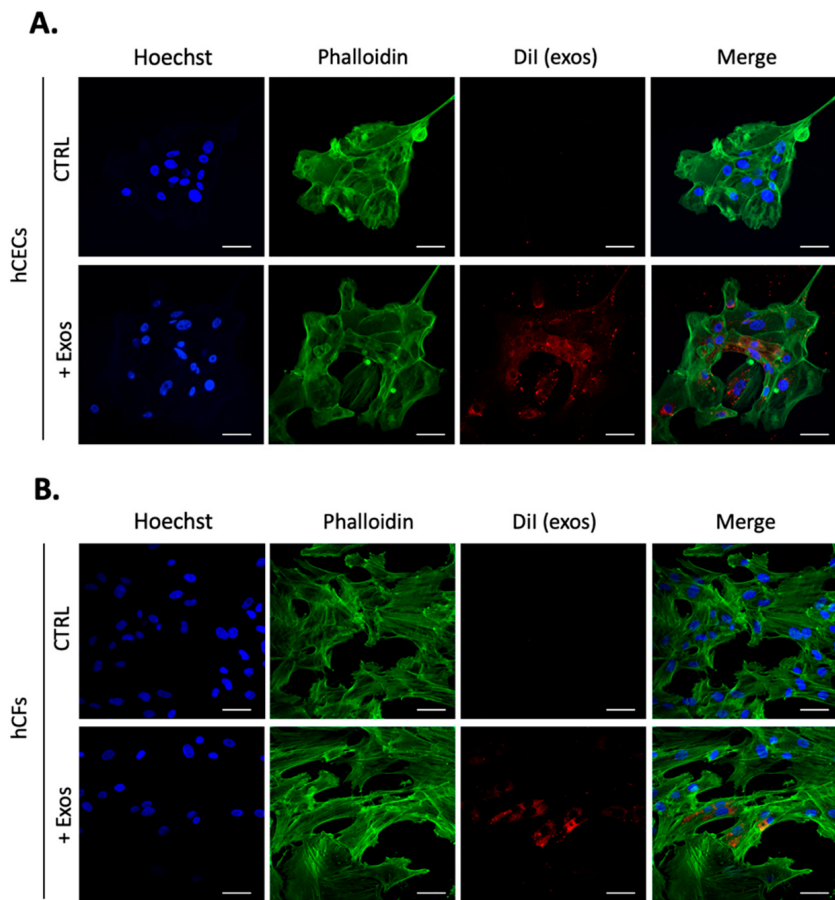
**Figure 1. Cont.**



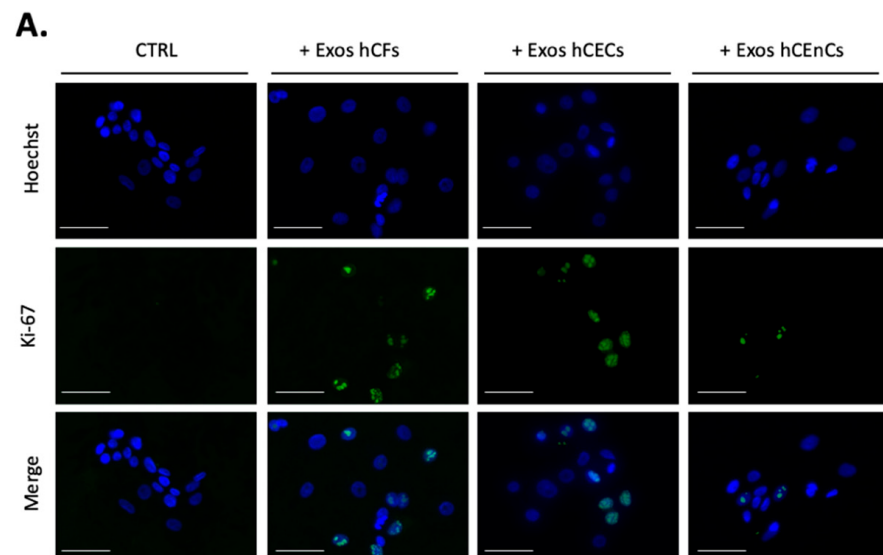
**Figure 1.** Characteristics of the exosomes isolated from the three corneal cell types. (A) TEM images of exosomes isolated from hCFs, hCECs and hCEnCs showing a range of exosomal size from 30–150 nm and a round morphology. Scale bars: 100 nm or 200 nm. (B) The diameter of the exosomes isolated from the three corneal cell types were analyzed by DLS. The means for the 10 measurements (repeated measures) were calculated and plotted on a graph. (C) Western Blot analysis of three specific exosomal markers (CD9, CD63 and CD81) as well as one negative marker (cytochrome c) in exosomes isolated from conditioned medium of hCFs, hCECs and hCEnCs. Corresponding cell lysate were used as a positive control for cytochrome c.

## 2.2. Human Corneal Exosomes Are Taken Up by hCECs and hCFs and Alter Their Growth Properties

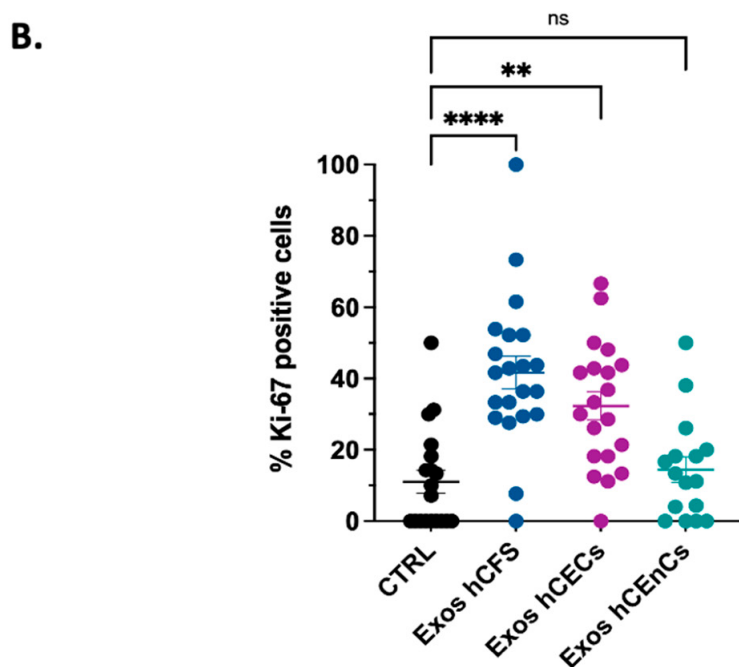
We next investigated the uptake of exosomes enriched from hCECs by both hCECs and hCFs grown as monolayers. After incubation of cultured cells with DiI-labeled exosomes for 24 h, red fluorescent particles were observed throughout the cells' cytoplasm of both hCECs and hCFs (Figure 2). Cells staining with Alexa Fluor 488-conjugated phalloidin which selectively label F-actin revealed that exosomes appear to be located throughout the cytoplasm and occasionally concentrated around the nuclei. We next monitored expression of the proliferation marker Ki-67 in hCECs grown for a period of 48 h with or without addition of exosomes (Figure 3). The addition of exosomes from hCECs or hCFs significantly increased the proportion of Ki-67 positive cells to 33% and 40%, respectively compared to 10% in control hCECs. In contrast, only a slight increase in the percentage of Ki-67 positive cells (14%) was observed with exosomes from hCEnCs. We also monitored expression of the proliferation marker Ki-67, but in hCFs. The hCFs are known to be highly proliferative cells, which results in a high proportion of Ki-67 positive cells for control hCFs (around 78%). Addition of exosomes, from any corneal cell types did not significantly alter the already high percentage of Ki-67 positive cells in hCFs (Supplementary Figure S2).



**Figure 2.** Exosomes uptake in hCECs and hCFs. Exosomes were labeled with the lipophilic dye, Dil. Dil-labeled exosomes were incubated (direct addition to the culture medium) with either hCECs or hCFs for 24 h prior to fixation and immunofluorescence staining. HBS, which was used to resuspend exosomes, was used as control (CTRL). Cells were stained with phalloidin, which exhibits green fluorescence, dil-labeled exosomes appeared in red and nuclei (Hoechst staining of DNA) in blue. Panels (A,B) show representative images of dil-labeled exosomes uptake by hCECs and hCFs, respectively. Scale bars: 50  $\mu$ m.



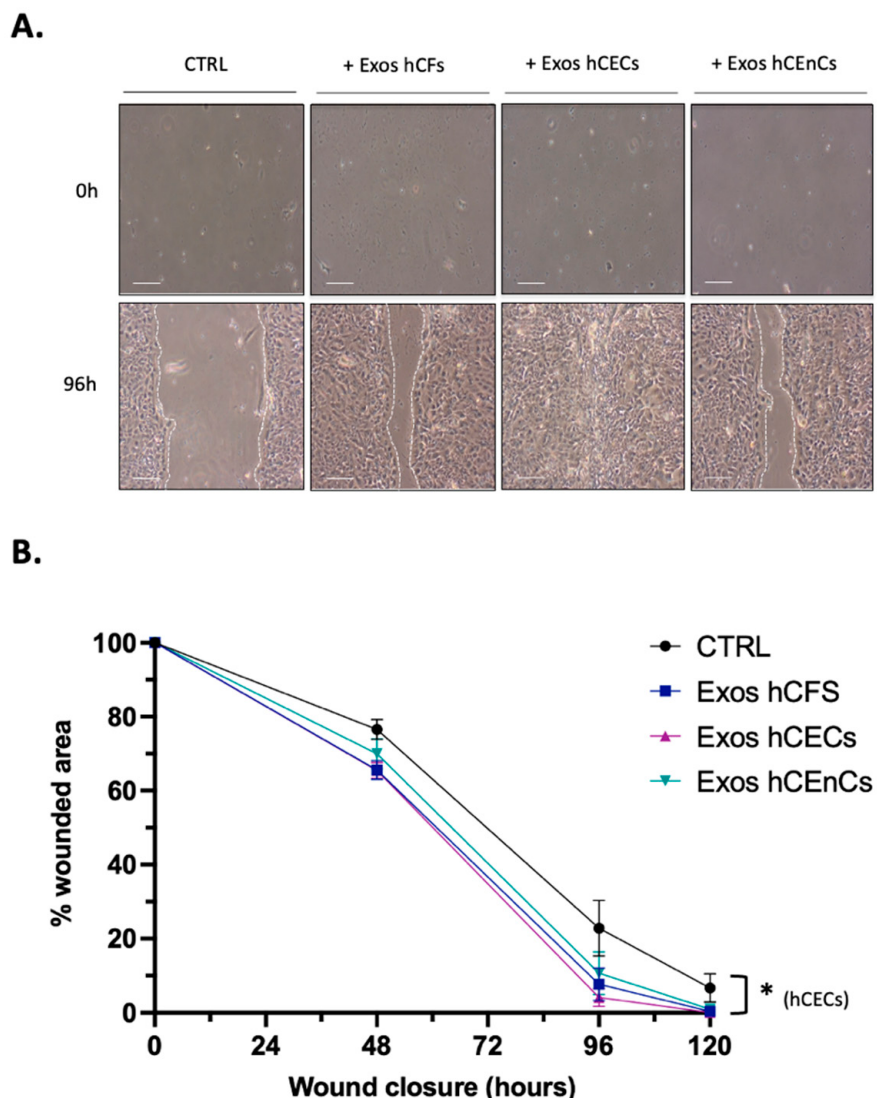
**Figure 3. Cont.**



**Figure 3.** Effect of exosomes from the three corneal cell types on hCECs proliferation. hCECs were incubated with 800–1000 µg exosomes isolated from medium of hCFs, hCECs and hCEnCs conditioned for 48 h. HBS was used as control (CTRL). Cells were fixed and Ki-67 was labeled by indirect immunofluorescence. Panel (A) shows representative images of Ki-67 expression in hCECs. Nuclei were counterstained with Hoechst 33258 reagent (blue). Scale bars: 100 µm. (B) The number of Ki-67 positive cells was calculated and plotted on graph. Between four and eight photos per condition were used for the counts. The data is expressed as the mean  $\pm$  SEM from three independent experiments on two different populations. \*\*  $p < 0.01$ , \*\*\*\*  $p < 0.001$ , ns: not significant.

### 2.3. Human Corneal Exosomes Accelerate Wound Closure of hCECs In Vitro

As exosomes from mesenchymal stem cells have been shown to significantly contribute to wound healing [42,55], we then wished to verify whether exosomes enriched from hCEnCs, hCECs and hCFs would similarly impact wound closure of hCECs in scratch wound assays. hCECs were selected for this experiment as most of the corneal wounds primarily involve the corneal epithelium [10,56]. Exosomes enriched from hCEnCs, hCECs and hCFs were therefore added individually to the culture media of scratch-wounded, confluent hCECs. Fresh media and exosomes were added every 48 h until the wound was completely closed for at least one condition. As shown on Figure 4A, wounds closed faster when exosomes (irrespective of their cells of origin) were added relative to control wounds that received no exosomes. Analysis of the percentage of wound area remaining over time revealed that addition of exosomes from hCECs, hCFs and hCEnCs reduced the wound surfaces at 96 h to 4.1%, 7.6% and 10.7%, respectively, and reached complete wound closure after 120 h. In contrast, for the controls, the wound surface was 22.8% at 96 h, 7% remained at 120 h and an additional 24 h incubation (to 144 h) was necessary for complete wound closure (Figure 4B). Therefore, the addition of corneal cells' exosomes accelerates scratch wound healing of hCECs monolayers.

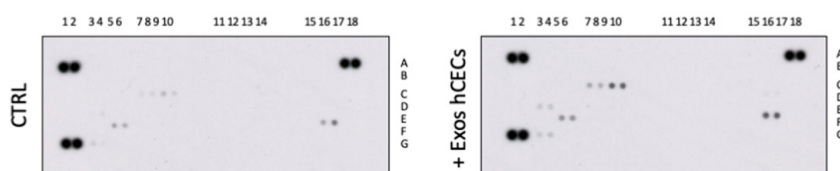
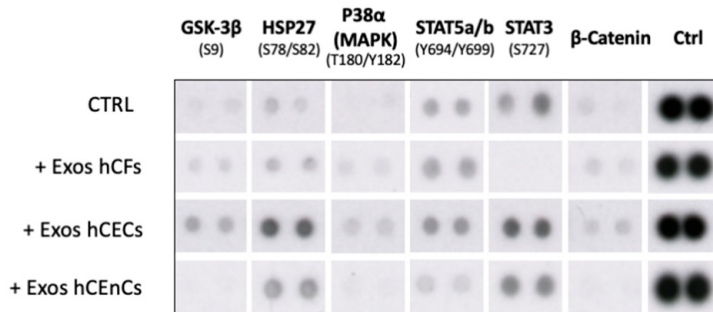
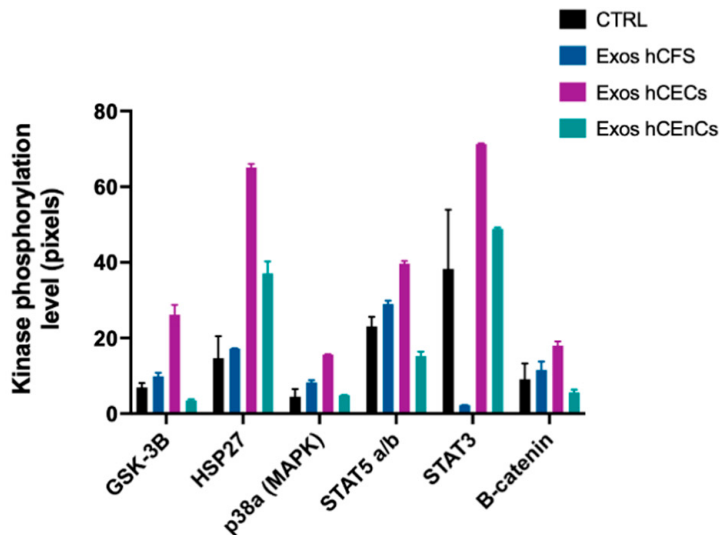


**Figure 4.** Impact of the three types of exosomes on wound closure of hCECs. (A) hCECs were grown as a monolayer and scratch-wounded. 800–1000 µg exosomes from each corneal cell type (hCFs, hCECs and hCEnCs) were separately administrated every 48 h and hCECs were allowed to recover. Scratches were photographed 0, 48, 96 and 120 h after wounding to monitor the healing process. As a negative control, hCECs were incubated with the vehicle alone (HBS). Scale bars: 200 µm. (B) The means of the wound surfaces remaining for each condition were calculated for each time interval and plotted on graph. Data is expressed as the mean ± SEM. For each time interval, results were compared to controls and the difference was considered statistically significant when \*  $p < 0.05$ .

#### 2.4. Signal Transduction Pathways Is Modified by Exosomes in hCECs

Interaction of exosomes with nearby cells has been shown to trigger the activation of intracellular signaling pathways such as JAK/STAT [57], mitogen-activated protein kinases (MAPKs) [58] or phosphatidylinositol-3OH kinase (PI3K)/Akt pathways [59]. To determine which from these exosome-activated signaling pathways contributes the most to corneal reepithelialization in our scratch-wounded model, phosphorylation levels of protein mediators from different pathways were examined using the human phospho-kinase proteome profiler array (Figure 5). Compared to controls (no added exosomes), the addition of hCECs exosomes led to a significant increase in the phosphorylation of GSK-3β, HSP27, p38α (MAPK), STAT5, STAT3 and  $\beta$ -catenin in hCECs (Figure 5B,C). The addition of hCFs exosomes activated the same mediators as those induced by hCECs exosomes except STAT3, whose activation was drastically reduced relative to control hCECs. Only HSP27

seeks its activation increased by the addition of exosomes from hCEnCs whereas that of GSK-3 $\beta$ , STAT5 and  $\beta$ -catenin was reduced. Therefore, exosomes from different corneal cells clearly have very distinctive impacts on the activation of cell signaling mediators in vitro.

**A.****B.****C.**

**Figure 5.** Impact of the exosomes isolated from the different corneal cell types on the phosphorylation of signal transduction mediators in hCECs. (A) Cells were cultured 48 h with hCFs-, hCECs-, hCEnCs-exosomes or the vehicle (HBS). Cell lysates prepared from hCECs were used as sources of proteins for the phosphokinase assays conducted as detailed in Section 4. The results obtained for hCECs exposed solely to the vehicle (HBS) or to hCECs exosomes are shown as examples. (B) Duplicate spots corresponding to the kinases (GSK-3 $\beta$ , p38 $\alpha$  (MAPK), STAT5a/b, STAT3,  $\beta$ -catenin) whose phosphorylation is the most altered in monolayer-cultured hCECs after the addition of exosomes from hCECs, HCFs or hCEnCs. hCECs exposed only to the vehicle were used as negative control (CTRL). (C) The phosphorylation level (in pixels) for each spot was determined with the ImageJ Software and plotted on graph. One of two representative experiments conducted using two distinct populations of hCECs is shown.

## 2.5. Exosomes Modify the Gene Expression Pattern in a Cell-Specific Manner

We next exposed near confluent hCECs (Figure 6), hCFs (Supplementary Figure S3) and hCEnCs (Supplementary Figure S6) to exosomes isolated from all three cell-types and conducted gene profiling analyses on microarrays using total RNAs isolated from both the negative controls and from exosomes-exposed hCECs, hCFs and hCEnCs. A scatter plot analysis of the 60,000 different transcripts contained on the arrays indicated that only a limited number of genes have their level of expression modified by the addition of exosomes in hCECs, as indicated by the values of the regression curves ( $R^2 = 0.9864$ , 0.9791 and 0.9824 for hCECs exposed to hCECs, hCFs, and hCEnCs exosomes, respectively; Figure 6A). Consistent with these results, 534, 255 and 350 genes were found to be differently regulated by more than a 2-fold factor between control hCECs and hCECs exposed to hCECs-, hCFs- or hCEnCs-derived exosomes, respectively. Interestingly, only 82 genes (which represents 15%, 32% and 23% of all the genes differentially regulated by the hCECs, hCFs and hCEnCs exosomes, respectively) were commonly modified by the three types of exosomes (Figure 6B).

Conducting a similar analysis for hCFs yielded values for the regression curves of 0.9727, 0.9801 and 0.9859 for hCFs exposed to hCFs, hCECs and hCEnCs exosomes, respectively (Supplementary Figure S3A). In addition, 688, 885 and 438 differently regulated genes were identified between control hCFs and hCFs exposed to hCECs-, hCFs- and hCEnCs-derived exosomes, respectively, of which 110 genes were commonly modified by the three types of exosomes (which represents 16%, 12% and 25% of all the genes differentially regulated by the hCECs, hCFs and hCEnCs exosomes, respectively) (Supplementary Figure S3B). Finally, hCEnCs exhibited the most perturbed transcriptomic profile upon addition of exosomes, with 1169, 544 and 1007 differentially regulated genes identified between control hCEnCs and hCEnCs exposed to hCECs-, hCFs- and hCEnCs-derived exosomes, respectively. Of all these genes, 229 were found to be modified by all types of exosomes (which represents 20%, 42% and 23% of all the genes differentially regulated by the hCECs, hCFs and hCEnCs exosomes, respectively) (Supplementary Figure S6B). Most interestingly, none of the genes identified as commonly modified by all three types of exosomes were common between hCECs (82 genes), hCFs (110 genes) and hCEnCs (229 genes) (Figure 6C). This result therefore clearly established the strong cell type-specific impact that corneal exosomes exert on the transcriptomic profile of corneal cells (hCECs, hCFs or hCEnCs) with which they interact.

We next examined the data files from the microarrays to sort out only the 50 genes whose expression is the most differentially regulated in hCECs that have been exposed to exosomes enriched from hCECs, hCEnCs and hCFs relative to cells unexposed to exosomes. Examination of Figure 7 indicates that 19 genes among the 50 most differentially regulated genes between controls and hCECs grown hCECs-, hCEnCs- or hCFs-exosomes are not just common to one another but also similarly modified in all conditions: the expression of 18 of these genes (indicated in red) was drastically reduced whereas that of one gene (indicated in blue) was increased. The same exercise was conducted for hCFs and hCEnCs that have been exposed to exosomes isolated from all three corneal cell-types and heatmaps of the 50 most differentially regulated genes were generated (Supplementary Figures S4 and S7, respectively). Similarly, 8 and 16 genes had their expression strongly reduced in hCFs and hCEnCs, respectively (named in red on Supplementary Figures S4 and S7), when they are grown in the presence of exosomes from either hCECs, hCFs or hCEnCs.

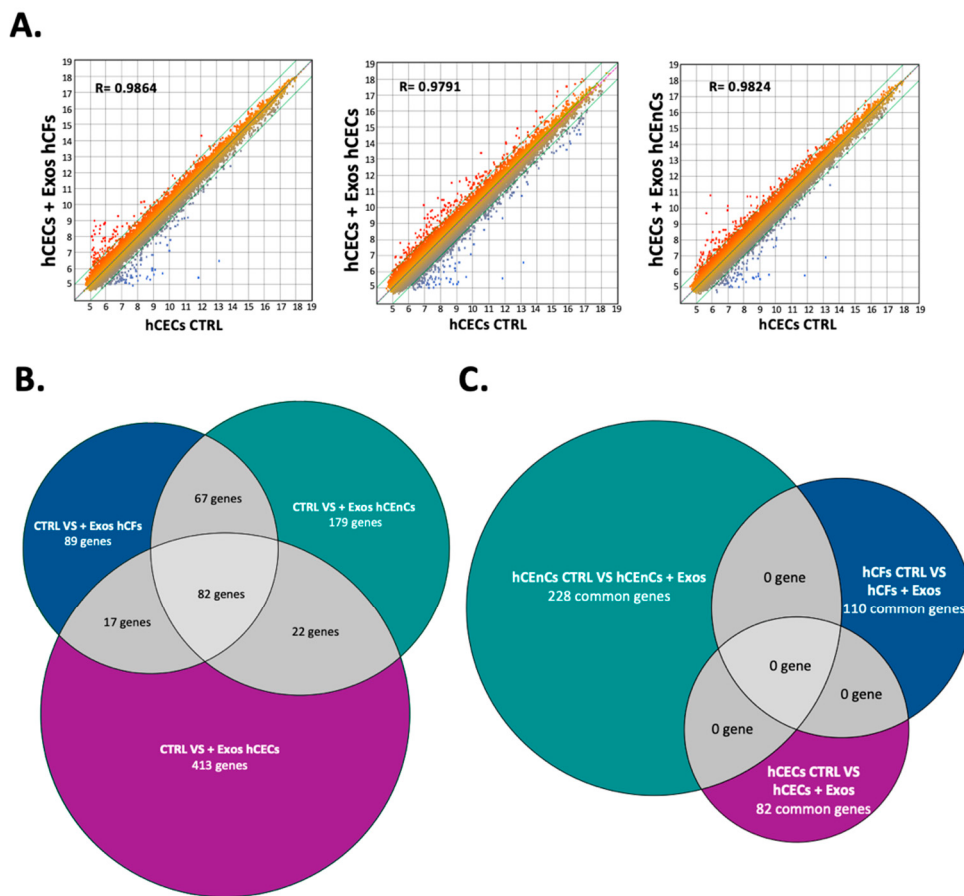


**Figure 6.** Microarray analysis of the gene expression pattern of hCECs cultured in the presence of hCFs-, hCECs- or hCEnC-exosomes. (A) Scatter plot of  $\log_2$  of signal intensity from 60,000 different targets covering the entire human transcriptome of hCECs + Exos hCFs (first graph), hCECs + Exos hCECs (second graph) or hCECs + Exos hCEnCs (third graph) in the y-axis as a function of hCECs CTRL (no added exosomes) in the x-axis. (B) Analysis of commonly regulated genes in hCECs. Venn diagram depicting the number of genes differently regulated by at least a two-fold factor between hCECs CTRL and hCECs + Exos hCFs (upper left; 89 genes); hCECs CTRL and hCECs + Exos hCECs (bottom; 413 genes) and those specific to the hCECs + Exos hCEnCs condition (upper right; 179 genes). Differently regulated genes shared between two groups are indicated at the intersections (17, 22 and 67 genes) and differently regulated genes common for three groups are indicated in the middle (82 genes). (C) Analysis of differentially regulated genes that are common following exposure to exosomes from each of the three different corneal cell types. In this Venn diagram, each circle indicated the number of genes differentially regulated by at least two-fold in hCFs, hCECs and hCEnCs exposed to exosomes from the three different sources. As shown in the panel (B), 82 genes are commonly differently regulated in hCECs CTRL vs. hCECs + Exos (from any source). As for hCEnCs and hCFs, there are respectively, 228 genes (upper left) and 110 genes (upper right) that are commonly differently regulated. All these genes are unique to a given cell population, none of those genes are shared between the three corneal cell types (middle; 0 gene).

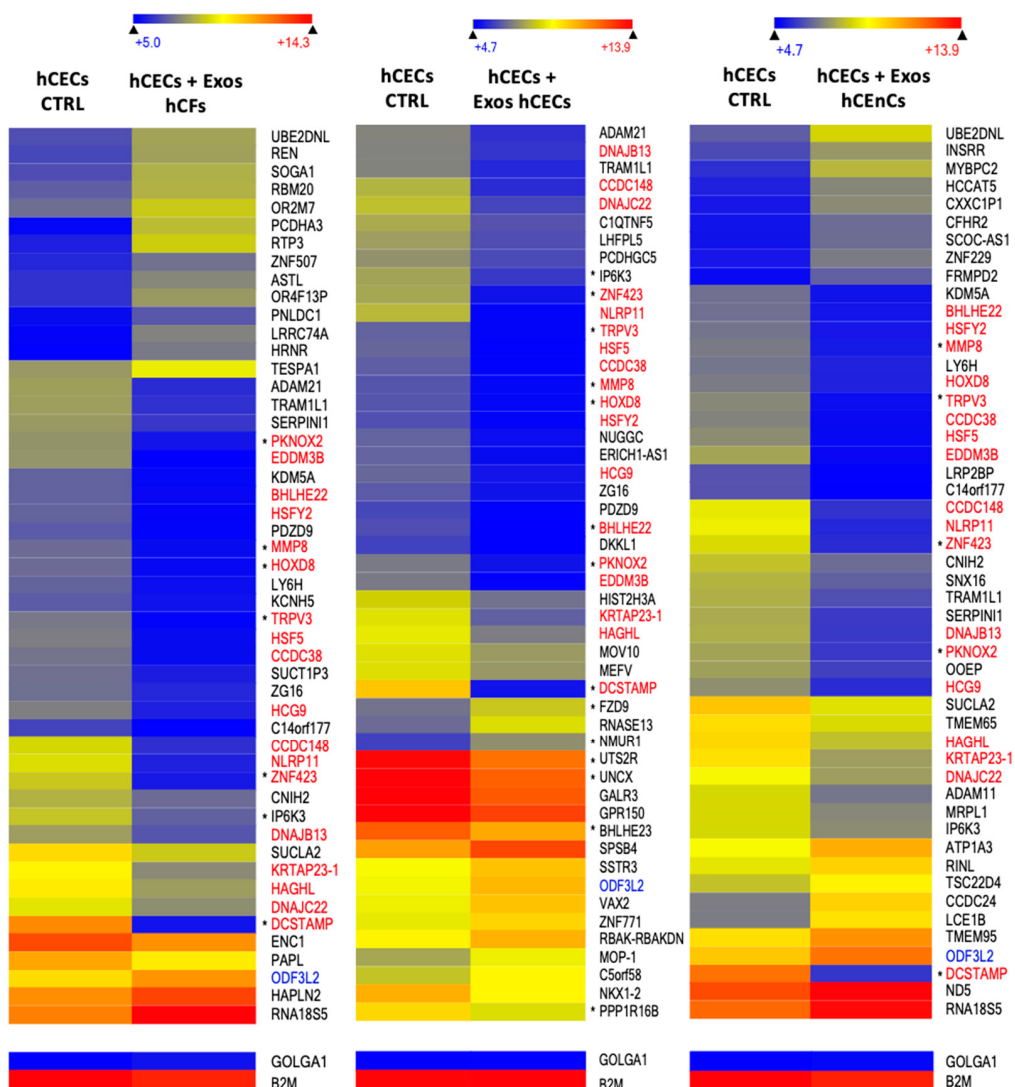


**Figure 7.** Gene expression pattern of hCECs cultured in the presence of hCFs-, hCECs- or hCEnC-exosomes. Heatmap representation of the 50 most differentially regulated genes in hCECs CTRL (no added exosomes) against hCECs + Exos hCFs (first heatmap), hCECs + Exos hCECs (second heatmap) or hCECs + Exos hCEnCs (third heatmap). Gene names indicated in red correspond to genes whose transcription are commonly downregulated in all three conditions whereas those in blue are upregulated. An asterisk placed before the gene name indicates that this gene has been associated with at least one function of interest in the IPA analysis. Microarray data for the golgin subfamily A member 1 (GOLGA1) and  $\beta$ 2-microglobulin (B2M) housekeeping genes that are expressed, respectively, at low and very high levels in all cell types are also shown.

#### 2.6. In Silico Prediction of Biological Functions Affected by Exosomes in hCECs and hCFs through Gene Interaction Network Analyses

We next perform a differential expression analysis on the microarray linear expression data from hCECs, hCFs and hCEnCs cultured in the presence of exosomes from either hCECs, hCEnCs or hCFs. We identified a total of 125, 333 and 390 differentially expressed genes between hCECs, hCFs and hCEnCs cultured with the three exosome types, respectively (adjusted  $p$ -value  $< 0.05$  and  $FC \geq 3$ ). We then uploaded the results from these analyses into the Ingenuity Pathway Analysis (IPA) software to be further analyzed. IPA's statistical algorithms and curated knowledge database can be used to predict what and how biological functions are likely to be influenced when provided with data from a differential expression analysis. We thus selected four biological functions of interest,

“proliferation”, “differentiation”, “migration” and “immune response” of hCECs (Figure 8), hCFs (Supplementary Figure S5) and hCEnCs (Supplementary Figure S8), to which we connected all the differentially expressed genes that were linked to these functions according to the database. We then used IPA to examine how these genes interacted and to computationally predict how the resulting networks affected the biological functions of interest. Given our microarray data analysis, IPA predicted that hCECs cultured in the presence of exosomes from the three corneal cell types (hCECs, hCEnCs and hCFs) would proliferate and migrate more than control hCECs while, in the meantime, they would differentiate less (Figure 8). Many of the 50 most differentially expressed genes (especially in hCECs exposed to exosomes isolated from hCECs) were also recognized by IPA to impact on the different cellular processes analyzed (gene names indicated by an asterisk in Figures 7, S4 and S7). As for hCECs, analysis of the IPA data also suggest that the three types of exosomes should prompt proliferation and migration of hCFs. However, the lack of any significant difference in the expression of the proliferation marker Ki-67 (Supplementary Figure S2) does not support the IPA data. In addition, the immune response is expected to be stimulated by the addition of hCECs and hCEnCs exosomes but inhibited by that of hCFs exosomes (Supplementary Figure S5). The scenario became quite different in hCEnCs as the IPA analysis suggested that all three types of exosomes should interfere with endothelial cell proliferation. In addition, IPA data indicate that upon addition of exosomes, migration, differentiation and immune response in endothelial cells are going in various directions depending on the cell type from which the exosomes originate (Supplementary Figure S8).

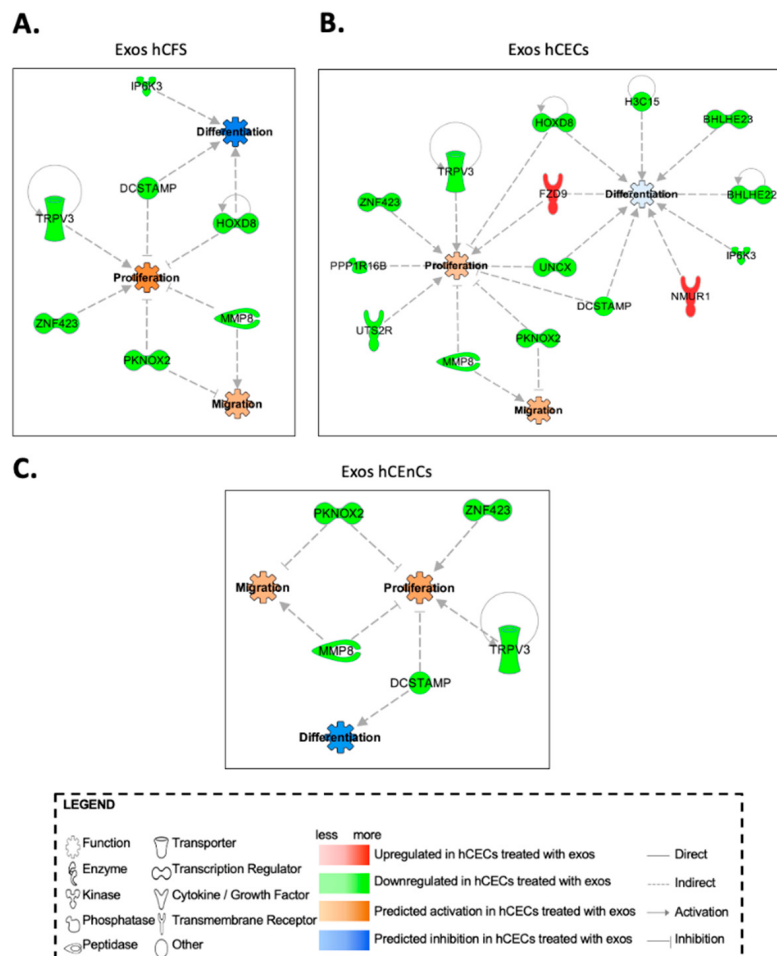


**Figure 8.** IPA generated interactome derived from differentially expressed genes in hCECs when supplemented with hCFs—(A), hCECs—(B) and hCEnCs—(C) exosomes. Computationally predicted biological functions of interest (proliferation, migration and differentiation) are identified with bold

labels and colored either orange or blue depending on whether they are predicted to be activated or inhibited respectively in cultures supplemented with exosomes. Differentially expressed genes present in our datasets are labeled with non-bold text and are colored either green or red depending on whether they were up- or downregulated respectively in cultures supplemented with exosomes. Lines indicate gene—gene and gene—function relationships (full lines for direct relationships and dotted lines for indirect ones) based on IPA's database. Functions are indicated in bold.

### 3. Discussion

Three major different types of extracellular vesicles have been recognized based on their respective mechanism of biogenesis: exosomes, ectosomes (including microvesicles and oncosomes, ranging in size between 100 nm to 10  $\mu\text{m}$ ) and apoptotic bodies (ranging in size between 1 to 5  $\mu\text{m}$ ). Exosomes are lipid bi-layer vesicles that originate from intracellular multivesicular bodies [38,60] and whose size vary from one study to another but are generally viewed as within 30 to 150 nm in diameter. Exosomes are very effective cell-to-cell intermediates that can deliver a whole array of compounds such as lipids, proteins and nucleic acids (including both mRNA and miRNA) [61–65]. They can be derived from various biological fluids such as blood, amniotic fluid, breast milk, synovial fluid, ascites and pleural effusions [66] or secreted by a large variety of cells such as fibroblasts, immune cells (both B and T cells), dendritic, neuron and intestinal cells, stem cells as well as cancer cells (reviewed in [66,67]). Exosomes also proved particularly promising at improving wound healing, especially for the skin [68–70]. By exploiting an epithelial debridement mouse model, Samaeekia et al. nicely demonstrated that exosomes derived from human corneal mesenchymal stromal cells could accelerate the wound closure of human corneal epithelial cells *in vitro* as well as *in vivo* [42]. Other recent studies have also highlighted the role of corneal-derived exosomes in corneal wound healing [41,71]. In the present study, we enriched exosomes from the three main cell types (epithelial, stromal and endothelial cells) of the human cornea and evaluated their capacity at modifying reepithelialization of human corneal epithelial cells in a monolayer scratch wound healing model. We demonstrated that all types of exosomes were efficiently taken up by hCECs, hCFs and hCEnCs and that they impacted on many biological functions of the recipient cells, such as proliferation and wound healing. We also found that exosomes from hCECs, hCFs and hCEnCs profoundly alter the transcriptomic profile of all three corneal cell types in a cell type-specific manner *in vitro*.

Characterization of EVs samples is a crucial, yet challenging step. Our results show clear size differences in the populations of exosomes between the three different types of cells, which ranged from 67 nm for exosomes enriched from hCFs, to 135 nm with those enriched from hCECs. TEM images also show EVs of different sizes ranging approximately from 50 to 150 nm. Variations in exosomes diameter is not uncommon as Rashid et al. reported they can vary from 98 to 140 nm in those released by human embryonic kidney 293 (HEK293), myeloid-derived suppressor cells (MDSCs) and endothelial progenitor cells (EPCs) [72]. In addition, the mean exosome diameter of human induced pluripotent stem cells (iPSCs) was found to be of 86 nm [73] whereas that of both adipose-derived stem cells (ADSCs) and human foreskin fibroblasts averaged 134 and 142 nm, respectively [74]. Tetraspanins is a family of transmembrane proteins that allow association with other members of the family and with other proteins to generate dynamic membrane domains. Traditionally, several members of this family, especially CD63, CD9 and CD81 were known to be highly enriched in exosomes from virtually any cell type and are commonly used as markers for exosomes identification, quantitation, or purification [75], although irregularities in their respective expression has recently been reported [76]. In our present study, all three exosome markers were found to be expressed by hCECs and hCFs exosomes but not by hCEnCs that were positive for CD63 and CD9 but not for CD81. However, and as reported by Garcia-Martin et al., the lack of CD81 expression in our endothelial exosomes is not unique as this marker was barely detectable in SVEC endothelial cells relative to

CD63 [76]. However, these types of tetraspanins have also been identified in other types of EVs, which highlights the complexity of finding a unique exosomal marker [77].

One clear finding is that human corneal exosomes are taken up by hCECs and hCFs in culture. Interestingly, exosomes' uptake appears to be more noticeable in hCECs compared to hCFs. This observation may be due to the cell distribution and level of confluence of the culture. Furthermore, the internalization process, the rate at which it occurs, and the intracellular fate of exosomes could also greatly vary depending on the cell type on which they are deposited. Once internalized, exosomes have clear effects on the biological functions of the target cells. Indeed, exosomes enriched from all types of corneal cells impacted to varying degrees on hCECs proliferation in the following order: hCFs > hCECs > hCEnCs (4-, 3.3- and 1.4-fold increase in Ki-67 positive cells, respectively). In addition, those purified from hCECs and hCFs were also those that impacted the most on wound closure of scratch-wounded hCECs. However, it is presently difficult to precisely determine the reasons why exosomes enriched from different cell types may have distinctive impacts on wound healing. We can assume that this is probably due, at least in part, to the differences inherent to each type of exosome, such as their cargo composition and the membrane receptors present at their surface. Moreover, some of our results might help understand them partly. Indeed, compared to controls (no added exosomes), addition of exosomes isolated from hCEnCs completely abolished the phosphorylation of glycogen synthase kinase 3 $\beta$  (GSK-3 $\beta$ ), p38 $\alpha$  (MAPK) and  $\beta$ -catenin in hCECs, whereas those isolated from hCECs and hCFs considerably increased activation of these signal transduction mediators. This is consistent with the fact that signal transduction through the GSK-3 $\beta$ / $\beta$ -catenin pathway is abundantly documented to promote proliferation in a large variety of cell types [78–82]. Not surprisingly, the GSK-3 $\beta$ / $\beta$ -catenin pathway is involved in the progression and invasiveness of many types of cancers [83–87]. Phosphorylation of  $\beta$ -catenin by GSK-3 $\beta$  targets  $\beta$ -catenin for ubiquitination and subsequent degradation [88,89]. Most interestingly, an intracellular signal transduction cascade involving p38 $\alpha$  (MAPK), GSK-3 $\beta$  and  $\beta$ -catenin has also been reported [90,91] in which p38 $\alpha$  (MAPK) inactivates GSK-3 $\beta$  by phosphorylation of its carboxy terminal end, leading to the activation of  $\beta$ -catenin [92]. In the eye, activation of p38 $\alpha$  (MAPK) was found to increase permeability of endothelial cells treated with VEGF [90]. In addition, in both primary and SV40-transformed human corneal epithelial cells, expression of the cornified envelope protein small proline-rich protein 1B (SPRR1B), a biomarker for squamous metaplasia, has been shown to be regulated by p38 $\alpha$  (MAPK) signaling through a cytokine-induced pathway [93]. Interestingly, adiponectin, a secreted protein produced mainly by adipose tissues that exerts its regulatory influences by binding its corresponding receptors (AdipoR1 and AdipoR2), has been reported to regulate  $\beta$ -catenin signaling in both cementoblasts and hippocampal neural stem/progenitor cells essentially by inactivating the GSK-3 $\beta$  kinase activity, a process that also involves activation of p38 $\alpha$  (MAPK) [91,94]. Adiponectin protects various organs and tissues through a yet not fully understood pleiotropic action. It exists in the circulation under three oligomeric complexes: a ~70 kDa low-molecular-weight (LMW) trimer, a ~140 kDa medium-molecular-weight (MMW) hexamer, and a ~300 kDa high molecular weight (HMW) oligomer containing more than 18 monomers [95,96].

To our knowledge, no study ever investigated the expression/secretion of adiponectin and its AdipoR1/R2 receptors in the human cornea. However, a detailed analysis of the hCECs microarray data we accumulated over the years indicated that although the adiponectin transcript was expressed only at very low levels in these cells, they do, however, strongly express both the AdipoR1 and AdipoR2 receptors mRNA transcripts (Supplementary Figure S9), indicating that they should be capable of responding to alterations in the plasma level of adiponectin. Most interestingly, the murine lacrimal glands were reported to express both adiponectin and adipoR2 mRNA [97] indicating that besides the blood, tears may as well represent a source of secreted adiponectin for hCECs. As a further support for the presence of AdipoR1/R2 in corneal epithelial cells, topically administered adiponectin proved effective to reduce inflammation of the ocular surface in a mouse

model of experimental dry eye [98] and corneal neovascularization in a rabbit [99]. It also increased epithelial migration and improved clinical signs and inflammation on the ocular surface after alkali burn, suggesting that adiponectin can promote wound healing in the cornea [100]. A recent proteomic study conducted on the protein cargo of exosomes released by different types of cultured cells provided evidence that HMW adiponectin was present at the surface of the exosome membrane [76]. Although we did not investigate whether our corneal exosomes do transport HMW adiponectin at their surface, such a location would, however, facilitate its interaction with its AdipoR1/R2 receptors and lead either to activation of p38 $\alpha$  (MAPK) or to stimulation of endocytosis and cargo delivery through vesicle internalization [101].

HSP27, another mediator that was also increased in hCECs upon addition of exosomes derived from hCECs, has also been linked to cellular proliferation. HSP27 is a small, ubiquitous heat shock protein that belongs to the group of molecular chaperones, which respond to various environmental stresses. HSP27 has been found to be overexpressed in various types of cancers [102,103], where it works as a balance regulator between cell death and survival. In a recent study, HSP27 has been found to promote the epithelial-to-mesenchymal transition and proliferation in colorectal carcinoma cells [104]. HSP27 has also been found to inhibit apoptosis and promote malignant transformation of human bronchial epithelial cells [105]. These results highlight the important role of this mediator in proliferation and survival of epithelial cells. In the wound healing experiment shown on Figure 4A, all exosomes yielded a faster wound closure than the controls. Yet, those isolated from hCECs were distinguished from the others as they clearly yielded a faster closure of scratch-wounded hCECs, whereas exosomes from both hCFs and hCEnCs proved equally efficient. When one looks at the data from the phospho-kinase array (Figure 5B), the only kinase that is activated by all three types of exosomes is HSP27. Interestingly, HSP27 was clearly more activated by hCECs exosomes than by either hCFs or hCEnCs exosomes. As stated above, activation of HSP27 is well known to stimulate cell proliferation and adhesion. Furthermore, it has been shown to be a critical component of the STAT3/HSP27/p38 $\alpha$  (MAPK)/Akt survival pathway that also involves phosphorylation of the transcription factor STAT5 [106]. Interestingly, both STAT3 and p38 $\alpha$  (MAPK) were identified among the few mediators that also have their phosphorylation level increased in hCECs supplemented with hCECs exosomes (but not with those from hCFs (no activated STAT3), nor hCEnCs, (no activated p38 $\alpha$  (MAPK)). Consequently, we believe the faster wound closure observed when hCECs are added exosomes from hCECs might have resulted from the activation of the STAT3/HSP27/p38 $\alpha$  (MAPK)/Akt survival pathway and that such activation is disrupted by the lack of some important mediators (STAT3 or p38 $\alpha$  (MAPK)) when exosomes from either hCFs or hCEnCs are used.

The fact that none of the 82 genes identified as commonly differentially regulated in hCECs by hCECs-, hCEnCs- and hCFs-exosomes were among those also identified as differentially regulated in hCFs (110 genes) and hCEnCs (228 genes) by the same three types of exosomes is particularly interesting in that it suggests that their respective protein cargo do exert very distinctive, cell-type specific impact on the targeted cell's transcriptome. This is supported by the recent finding that despite exosomes isolated from various cell types do share common proteins, between 9 and 28% of their protein content is unique to each of them, as could be demonstrated by mass spectrometry and confirmed by immunoblotting [76]. This may explain, at least in part, why they are predicted (by IPA analyses) to differently affect the biological functions examined. From this striking result, we may also hypothesize that the bioactive molecules that the exosomes carry would not be what would have the most significant impact. Rather, what seems most significant is how the cells that receive the exosomes react to them, more particularly which receptors are triggered and which intracellular signaling pathways are activated. Each corneal cell type is indeed very distinct from one another, with striking differences both from an anatomical and functional point of view. Corneal epithelial cells act together to form a barrier that protects the cornea. These cells undergo constant renewal, going through several cycles

of proliferation before entering terminal differentiation. Stromal fibroblasts are elongated, highly proliferative cells in vitro that maintain stromal homeostasis by participating in the collagens, glycosaminoglycans and matrix metalloproteinases (MMPs) production. Corneal endothelial cells are polygonal cells that express a high density of sodium-potassium pumps ( $\text{Na}^+$ ,  $\text{K}^+$ -ATPase) at their basolateral membrane. These ion pumps allow the endothelial cells to carry out their main function, i.e., maintaining the state of deturgescence (state of partial dehydration) of the corneal stroma, which is necessary in order to allow optimal light transmission. Unlike corneal epithelial cells, corneal endothelial cells do not proliferate in vivo [107]. Not surprisingly, the three different corneal cell types do not show the same sensitivity and reactivity towards a large number of factors, including growth factors, cytokines and extracellular matrix proteins. For example, high affinity EGF receptors (EGFR) are known to be present on the surface of epithelial and endothelial cells, but absent on stromal keratocytes [108]. Among the other notable differences, the EGFR, IL-1R, PDGF-R receptors are mainly or exclusively expressed by fibroblasts and the KGFR and c-met receptors, in contrast, are mainly expressed by epithelial cells [109], which may be elevated during wound healing [110]. The integrin expression profile is also significantly different between the three corneal cell types with the heterodimers  $\alpha 6\beta 4$  and  $\alpha v\beta 6$  being exclusively identified in the epithelium and the heterodimer  $\alpha 4\beta 1$  in the fibroblasts [111]. All those differences are likely to lead to cell specific signal integration and therefore are likely to contribute to the distinctive, cell-type specific impact that exosomes exert on the targeted cell's transcriptome.

It is worthy noticing that in a biological context, communication between the three layers of the cornea through exosomes' release could be restricted in some ways. Indeed, exosomes from hCECs are less likely to reach and impact hCEnCs and vice versa due to the physical distance and the physiological barriers that separate these two layers. Studies in tissue-engineered corneal models and in ex vivo rabbit corneas have demonstrated that EVs can be visualized within the collagen matrix of the stroma and within the corneal endothelium [44]. EVs also appear to penetrate the Descemet's membrane [44], supporting the idea of a stromal-endothelial cell communication. As for the basement membrane, it appears to limit the diffusion of EVs to the stroma. However, if the BM is disrupted, as it often occurs in the case of corneal epithelial injury, EVs may gain access to the underlying stroma and therefore impact on corneal fibroblasts [41,112]. Consequently, the most relevant results, from a biological point of view, concern the impact of hCECs exosomes on hCFs and vice versa and the impact of hCFs exosomes on hCEnCs and the other way around.

In summary, we demonstrated that the three corneal cell types indeed release EVs that could be effectively enriched by differential ultracentrifugation. Characterization of our samples allows determining that the enriched EVs were positive for exosomal markers CD63, CD9 and CD81 and range in size from 50 to 150 nm in diameter, supporting the idea that our samples are mainly composed of exosomes. In our study, exosomes turned out to be real functional entities, since once internalized, they could stimulate cell proliferation of hCECs. They also demonstrated an exciting potential to enhance corneal epithelial wound healing in a monolayer model. Finally, cornea-derived exosomes also had a cell-type specific impact on the gene expression pattern of hCECs with the differential regulation of genes whose encoded protein products are involved in proliferation, migration and differentiation, three functions that are of great importance in the wound healing process.

#### 4. Materials and Methods

This study was conducted in accordance with our institution's guidelines and the Declaration of Helsinki. The protocols were approved by the CHU de Québec—Université Laval hospital and Université Laval Committees for the Protection of Human Subjects (ethic code: DR-002-955, protocol renewal approved on 21 February 2022).

#### 4.1. Cell Isolation and Culture

hCECs, hCFs and hCEnCs were isolated from the cornea of normal human eyes (obtained from the Banque d’Yeux Nationale of the Centre Universitaire d’Ophtalmologie; CHU de Québec, Hôpital du Saint-Sacrement, Québec, QC, Canada). To isolate hCEnCs, the Descemet membrane was carefully peeled off and incubated overnight in culture medium at 37 °C. It was then digested with EDTA 0.02% buffered solution (Sigma-Aldrich, St. Louis, MO, USA) for 1 h. Cells were detached by pipetting up and down with a flamed-polished pipette [113]. hCEnCs were then seeded on fibronectin/collagen (FNC)-coated plastic culture dishes and grown until they reached confluence in a proliferation medium (Opti-MEM-I medium supplemented with 8% fetal bovine serum, 5 ng/mL epidermal growth factor, 0.08% chondroitin sulfate, 20 µg/mL ascorbic acid and 100 IU/mL of penicillin and 100 µg/mL of streptomycin). The culture medium was then replaced with a maturation medium (Opti-MEM-I medium supplemented with 8% fetal bovine serum and penicillin/streptomycin) when hCEnCs reached confluence and were grown further for an additional 7 to 28 days [114]. hCEnCs were used between passages 2 and 6.

To isolate hCECs and hCFs, post-mortem corneas were incubated with dispase (Roche Diagnostics, Laval, QC, Canada) in HEPES buffer (MD Biomedicals, Montreal, QC, Canada) overnight at 4 °C to separate the epithelium from the stroma. The stroma was then cut into small pieces and incubated with collagenase H (Sigma-Aldrich) until the ECM was fully digested by the enzyme. hCECs were treated with trypsin for 15 min at 37 °C to separate the cells from each other. hCECs were grown in DH medium (Dulbecco–Vogt modification of Eagle’s medium with Ham’s F12 in a 3:1 ratio supplemented with 5% FetalClone II serum, 5 µg/mL of insulin, 0.4 µg/mL of hydrocortisone, 10 ng/mL of epidermal growth factor, 0.212 mg/mL of isoproterenol hydrochloride (Sigma-Aldrich, Oakville, ON, Canada), antibiotics (100 IU/mL of penicillin, and 25 µg/mL of gentamycin)) on lethally irradiated human fibroblasts feeder layers (iHFL) until they reached confluence [115]. hCECs were used between passages 1 and 4. hCFs were grown in DME medium (Dulbecco–Vogt modification of Eagle’s medium supplemented with 10% fetal calf serum and antibiotics). hCECs and hCFs were used between passages 2 and 6. All cells were grown under 8% CO<sub>2</sub> at 37 °C and culture medium was changed every 2 or 3 days.

#### 4.2. Exosome Enrichment

Exosomes were isolated by differential ultracentrifugation as previously described [116], with minor modifications. Approximately 48 h before the isolation of exosomes, the culture media of confluent hCFs, hCECs and hCEnCs were changed for culture media with exosome depleted-FBS (serum was depleted of exosomes using ultracentrifugation and filtration). Conditioned media were collected and subsequently centrifuged at 300× g for 10 min and 2000× g for 20 min to remove cells and large debris. The supernatant was then centrifuged at 21,000× g for 1 h 30 min at 4 °C to pellet larger microvesicles. For exosome enrichment, the supernatant was centrifuged at 100,000× g overnight at 4 °C. Each exosome pellet was resuspended in HEPES-Buffered Saline (HBS) and kept at 4 °C during the experimental procedure. For long time storage, exosomes were kept at –80 °C.

#### 4.3. Quantification of Exosomes

An estimate of the protein concentration of our samples was obtained using a NanoDrop 2000 spectrophotometer (Thermo Fisher Scientific, Mississauga, ON, Canada) at 280 nm.

#### 4.4. Electron Microscopy

Exosomes were fixed in 2.5% glutaraldehyde (Canemco, Lakefield, QC, Canada) and processed for transmission electron microscopy (TEM). Exosomes samples were diluted (1/100) and stained with 3% uranyl acetate for 20 s and left to dry overnight. Samples were visualized using a JEOL JEM-1230 (Tokyo, Japan) transmission electron microscope at 80 kV.

Prior to observation, the grids were hydrophilized with an X-Cite 120Q UV lamp (Excelitas Technologies, Waltham, MA, USA) for a maximum of 1 h to minimize aggregation.

#### 4.5. Dynamic Light Scattering (DLS)

The sizes of the isolated exosomes were determined by Dynamic Light Scattering using NanoBrook Omni from Brookhaven Instruments Corporation (Holtsville, NY, USA). Exosomes' suspensions (500  $\mu$ L each) were added to disposable plastic cuvettes (#952010051), air bubbles were carefully removed, and measurements were recorded. The apparatus was set to an angle of 90° at 25 °C. After an equilibrium time of 2 min, 10 measurements of 120 s were performed for each sample and values were reported as Effective Diameter. Analysis of the size distribution was performed using the CONTIN algorithm.

#### 4.6. Western Blot Analyses

Western blots were conducted using total protein extracts prepared from exosomes samples isolated from hCFs, hCECs and hCECs. Exosomes were lysed with TNG-T lysis buffer (15 nM NaCl, 5 mM Tris-HCl, 1% Glycerol, 0.1% Triton X-100) supplemented with protease inhibitor cocktail (Sigma-Aldrich) and protein concentration was evaluated with the Bradford procedure. Western blots were conducted as described [117] using the following primary antibodies: mouse monoclonal antibodies against CD81 (1:1000; 349502, Biolegend, San Diego, CA, USA), CD9 (1:1000; 312102, Biolegend) and CD63 (1:1000; 353013, Biolegend) and a rabbit polyclonal antibody against Cytochrome-c (1:500; SC-7159 H-104, Santa Cruz Biotechnology, Dallas, TX, USA). A peroxidase-conjugated AffiniPure Goat antibody against either mouse or rabbit IgG (1:2500; 115-036-003, Jackson ImmunoResearch Laboratories, Baltimore, PA, USA) was used as a secondary antibody. Primary antibodies were incubated overnight at 4 °C. The secondary antibody was incubated for 90 min at room temperature. The blots were revealed using ECL Plus Western blotting detection system (Thermo Fisher Scientific Inc.).

#### 4.7. Exosomes Uptake

Cellular uptake of exosomes by hCECs and hCFs was assessed by confocal microscopy. Exosome were labeled with DiI fluorescent dye (1,1'-dioctadecyl-3,3',3'-tetramethylindocarbocyanine perchlorate; Thermo Fisher Scientific), a lipophilic membrane stain. Briefly, exosomes' suspensions (100  $\mu$ L each) were incubated with DiI dye for 20 min at 37 °C in the dark. Then labeled-exosomes were washed, collected and added to hCECs and hCFs cultures. Cells were incubated with labeled exosomes for 24 h prior to fixation in 4% formaldehyde. Prior to immunodetection, cells were permeabilized with 0.2% Triton X-100 for 10 min. Cell nuclei and actin filaments were counterstained with Hoechst reagent 33258 (1:100; Sigma) and phalloidin-Alexa 488 (1:200, Invitrogen, Carlsbad, CA, USA) respectively. Photos were taken with a confocal microscope (LSM 800; Zeiss, Toronto, ON, Canada).

#### 4.8. Ki-67 Immunofluorescences

hCECs were seeded in 24-well plates on coverslip glasses at  $2 \times 10^4$  cells/well in complete DH medium. At 6 h post-seeding, different types of exosomes (800  $\mu$ g) or vehicle alone (HBS; negative control) were added to cultures. Cells were incubated for 48 h at 37 °C before they were fixed in 4% formaldehyde. Cells were then permeabilized with 0.2% Triton X-100 for 10 min and incubated with the following primary antibody: mouse monoclonal antibody against Ki-67 (1:200, #556003, BD Biosciences, Franklin Lakes, NJ, USA). Samples were washed with PBS before addition of secondary antibody, peroxidase-conjugated AffiniPure Goat anti-mouse IgG488 (1:400, A11059, Invitrogen). All antibodies were diluted in PBS containing 1% bovine serum albumin. Cell nuclei were counterstained with Hoechst reagent 33258 (1:100; Sigma). Coverslips were mounted on glass slides with mounting medium and kept at 4 °C until observation with an epifluorescence microscope (Zeiss Axio Imager Z2 microscope; Zeiss Canada Ltd.). Samples were photographed with a numeric CCD camera (AxioCam MRM; Zeiss Canada Ltd.). Negligible background was

observed for controls (primary antibodies omitted). Number of Ki-67-positive cells was counted and expressed as a percentage of the total number of cells.

#### 4.9. Scratch Wound Assay

hCECs ( $1.86 \times 10^5$  cells) were plated with  $1.68 \times 10^5$  iHFL/cm<sup>2</sup> in 60 mm petri dish in DH medium. When cells reached confluence, a 1.3 cm-large  $\times$  5 cm-long scratch was created in the center of the plate using a policeman (Sarstedt, Nümbrecht, Germany) prior to addition of exosomes from the three corneal cell types (Exos hCFs, Exos hCECs, Exos hCEnCs; 800 µg) or HBS (negative control). Wound closure was monitored on triplicates, and photographs were collected at various time intervals (0, 48, 96 and 120 h). Fresh exosomes were added to the cultures at the time of media changes every 2 days. The wound surface over time was measured using the ImageJ software (version 2.1.0, Wayne Rasband, National Institute of Health (NIH), Bethesda, MD, USA).

#### 4.10. Phosphokinase Arrays

The relative levels of 37 different human phosphorylated protein kinases were determined using a membrane-based antibody array (R&D Systems, Minneapolis, MN, USA) according to the manufacturer's instructions. Briefly, equal amounts (300 µg) of cell lysates prepared from hCECs were incubated overnight with the phosphokinase array membrane. The membrane was then washed to remove unbound proteins and incubated with a mixture of biotinylated detection antibodies. Streptavidin-HRP and chemiluminescent detection reagents were applied, and the signal produced at each captured spot quantified using ImageJ (from Wayne Rasband, NIH). The intensity of each spot including the positive control was quantified and the background was subtracted.

#### 4.11. Gene Profiling

All microarray analyses were conducted by the CUO-Recherche gene profiling service (Québec, QC, Canada) as previously described [118,119]. Total RNA was isolated from hCECs, hCFs and hCEnCs exposed or not for 48 h to various populations of exosomes using the RNeasy Mini Kit (QIAGEN, Hilden, Germany) and its quality determined (2100 Bioanalyzer, Agilent Technologies, Santa Clara, CA, USA). Labeling of Cyanine 3-CTP labeled targets, their hybridization on a G4851A SurePrint G3 Human GE 8x60K array slide (Agilent Technologies) and data acquisition and analyses were all performed as previously reported [118]. All data generated from the arrays were analyzed by robust multi-array analysis (RMA) for background correction of the raw values. They were then transformed in Log2 base and quantile normalized before a linear model was fitted to the normalized data to obtain an expression measure for each probe set on each array. Scatter plots and heat maps were generated using the ArrayStar V4.1 (DNASTAR, Madison, WI, USA) software. All microarray data presented in this study comply with the Minimum Information About a Microarray Experiment (MIAME) requirements. (GSE # will be provided prior to publication).

#### 4.12. Bioinformatics and Ingenuity Pathway Analyses

The ArrayStar microarray differential linear expression data from hCFs, hCECs and hCEnCs grown either alone or in the presence of exosomes were uploaded to and analyzed with Ingenuity Pathway Analysis (IPA; QIAGEN Inc., <https://www.qiagenbioinformatics.com/products/ingenuitypathway-analysis>, accessed on 14 March 2022) software in order to compute and visualize causal gene interaction networks around selected cellular functions of interest in hCFs, hCECs and hCEnCs [120,121].

#### 4.13. Statistical Analyses

In Figures 3 and 4, Kruskal–Wallis and Mann–Whitney tests were employed to determine statistical significance for comparison of the groups in the Ki-67 immunofluorescence quantification and scratch assays.  $p < 0.05$  was considered significant. All data are expressed as mean  $\pm$  SEM.

**Supplementary Materials:** The following supporting information can be downloaded at: <https://www.mdpi.com/article/10.3390/ijms232012201/s1>.

**Author Contributions:** Conceptualization, S.L.G., L.G. and P.D.; methodology, P.D., R.B., C.C., G.L.-B. and V.R.; formal analysis, P.D.; writing—original draft preparation, P.D. and C.C.; writing—review and editing, S.L.G., L.G., V.R., V.J.M., S.P., F.G.-L. and S.C.; supervision, S.L.G. and L.G.; funding acquisition, S.L.G., L.G., V.J.M. and S.C. All authors have read and agreed to the published version of the manuscript.

**Funding:** This work was supported by a grant from the National Science and Engineering Research Council of Canada (NSERC; grant #RGPIN-2017-06123) to S.L.G. and the Quebec Cell, Tissue and Gene Therapy Network—ThéCell (a thematic network supported by the Fonds de recherche du Québec—Santé). The Banque d’yeux Nationale is partly supported by the Réseau de Recherche en Santé de la Vision from the FRQS. P.D. and C.C. were supported by studentships from the CIHR and the FRQS, respectively. L.G. is the recipient of a Tier 1 Canadian Research Chair on Stem Cells and Tissue Engineering and a Research Chair on Tissue-Engineered Organs and Translational Medicine of the Fondation de l’Université Laval.

**Institutional Review Board Statement:** Not applicable.

**Informed Consent Statement:** Not applicable.

**Data Availability Statement:** All microarray data presented in this study can be accessed at NCBI Gene Expression Omnibus (GEO# GSE215102; <https://www.ncbi.nlm.nih.gov/geo/query/acc.cgi?acc=GSE215102>, accessed on 9 October 2022).

**Acknowledgments:** The authors would like to thank Gabrielle Raiche-Marcoux, Ange Tchatchouang and Princia Anney for their technical assistance.

**Conflicts of Interest:** The authors declare no conflict of interest.

## References

- Lin, Y.B.; Gardiner, M.F. Fingernail-induced corneal abrasions: Case series from an ophthalmology emergency department. *Cornea* **2014**, *33*, 691–695. [CrossRef] [PubMed]
- Lee, S.Y.; Kim, Y.H.; Johnson, D.; Mondino, B.J.; Weissman, B.A. Contact lens complications in an urgent-care population: The University of California, Los Angeles, contact lens study. *Eye Contact Lens* **2012**, *38*, 49–52. [CrossRef] [PubMed]
- Hong, J.W.; Liu, J.J.; Lee, J.S.; Mohan, R.R.; Mohan, R.R.; Woods, D.J.; He, Y.G.; Wilson, S.E. Proinflammatory chemokine induction in keratocytes and inflammatory cell infiltration into the cornea. *Investig. Ophthalmol. Vis. Sci.* **2001**, *42*, 2795–2803.
- Ramakrishnan, T.; Constantinou, M.; Jhanji, V.; Vajpayee, R.B. Corneal metallic foreign body injuries due to suboptimal ocular protection. *Arch. Environ. Occup. Health* **2012**, *67*, 48–50. [CrossRef] [PubMed]
- Vemuganti, G.K.; Murthy, S.I.; Das, S. Update on pathologic diagnosis of corneal infections and inflammations. *Middle East Afr. J. Ophthalmol.* **2011**, *18*, 277–284. [CrossRef] [PubMed]
- Logothetis, H.D.; Leikin, S.M.; Patriankos, T. Management of anterior segment trauma. *Dis. Mon.* **2014**, *60*, 247–253. [CrossRef] [PubMed]
- Daniels, J.T.; Dart, J.K.; Tuft, S.J.; Khaw, P.T. Corneal stem cells in review. *Wound Repair Regen.* **2001**, *9*, 483–494. [CrossRef] [PubMed]
- Pokhrel, P.K.; Loftus, S.A. Ocular emergencies. *Am. Fam. Phys.* **2007**, *76*, 829–836.
- Gelston, C.D. Common eye emergencies. *Am. Fam. Phys.* **2013**, *88*, 515–519.
- Agrawal, V.B.; Tsai, R.J. Corneal epithelial wound healing. *Indian J. Ophthalmol.* **2003**, *51*, 5–15. [PubMed]
- Meek, K.M.; Knupp, C. Corneal structure and transparency. *Prog. Retin. Eye Res.* **2015**, *49*, 1–16. [CrossRef] [PubMed]
- Sta Iglesia, D.D.; Gala, P.H.; Qiu, T.; Stepp, M.A. Integrin expression during epithelial migration and restratification in the tenascin-C-deficient mouse cornea. *J. Histochem. Cytochem.* **2000**, *48*, 363–376. [CrossRef] [PubMed]
- Wilson, S.E.; Liu, J.J.; Mohan, R.R. Stromal–epithelial interactions in the cornea. *Prog. Retin. Eye Res.* **1999**, *18*, 293–309. [CrossRef]

14. Lee, J.S.; Liu, J.J.; Hong, J.W.; Wilson, S.E. Differential expression analysis by gene array of cell cycle modulators in human corneal epithelial cells stimulated with epidermal growth factor (EGF), hepatocyte growth factor (HGF), or keratinocyte growth factor (KGF). *Curr. Eye Res.* **2001**, *23*, 69–76. [CrossRef] [PubMed]
15. Lee, J.G.; Ko, M.K.; Kay, E.P. Endothelial mesenchymal transformation mediated by IL-1beta-induced FGF-2 in corneal endothelial cells. *Exp. Eye Res.* **2012**, *95*, 35–39. [CrossRef]
16. Roy, O.; Leclerc, V.B.; Bourget, J.M.; Theriault, M.; Proulx, S. Understanding the process of corneal endothelial morphological change in vitro. *Investig. Ophthalmol. Vis. Sci.* **2015**, *56*, 1228–1237. [CrossRef]
17. Keller, S.; Sanderson, M.P.; Stoeck, A.; Altevogt, P. Exosomes: From biogenesis and secretion to biological function. *Immunol. Lett.* **2006**, *107*, 102–108. [CrossRef]
18. Yeates, E.F.; Tesco, G. The Endosome-associated Deubiquitinating Enzyme USP8 Regulates BACE1 Enzyme Ubiquitination and Degradation. *J. Biol. Chem.* **2016**, *291*, 15753–15766. [CrossRef] [PubMed]
19. Meldolesi, J. Exosomes and Ectosomes in Intercellular Communication. *Curr. Biol.* **2018**, *28*, R435–R444. [CrossRef] [PubMed]
20. Kennedy, M.J.; Ehlers, M.D. Mechanisms and function of dendritic exocytosis. *Neuron* **2011**, *69*, 856–875. [CrossRef]
21. Lee, Y.R.; Kim, G.; Tak, W.Y.; Jang, S.Y.; Kweon, Y.O.; Park, J.G.; Lee, H.W.; Han, Y.S.; Chun, J.M.; Park, S.Y.; et al. Circulating exosomal noncoding RNAs as prognostic biomarkers in human hepatocellular carcinoma. *Int. J. Cancer* **2019**, *144*, 1444–1452. [CrossRef] [PubMed]
22. Hood, J.L.; San, R.S.; Wickline, S.A. Exosomes released by melanoma cells prepare sentinel lymph nodes for tumor metastasis. *Cancer Res.* **2011**, *71*, 3792–3801. [CrossRef]
23. Record, M.; Carayon, K.; Poirot, M.; Silvente-Poirot, S. Exosomes as new vesicular lipid transporters involved in cell-cell communication and various pathophysiologies. *Biochim. Biophys. Acta* **2014**, *1841*, 108–120. [CrossRef] [PubMed]
24. Pietrowska, M.; Funk, S.; Gawin, M.; Marczak, L.; Abramowicz, A.; Widlak, P.; Whiteside, T. Isolation of Exosomes for the Purpose of Protein Cargo Analysis with the Use of Mass Spectrometry. *Methods Mol. Biol.* **2017**, *1654*, 291–307. [PubMed]
25. Goetzl, E.J.; Mustapic, M.; Kapogiannis, D.; Eitan, E.; Lobach, I.V.; Goetzl, L.; Schwartz, J.B.; Miller, B.L. Cargo proteins of plasma astrocyte-derived exosomes in Alzheimer’s disease. *FASEB J.* **2016**, *30*, 3853–3859. [CrossRef] [PubMed]
26. Yun, J.; Han, S.B.; Kim, H.J.; Go, S.I.; Lee, W.S.; Bae, W.K.; Cho, S.H.; Song, E.K.; Lee, O.J.; Kim, H.K.; et al. Exosomal miR-181b-5p Downregulation in Ascites Serves as a Potential Diagnostic Biomarker for Gastric Cancer-associated Malignant Ascites. *J. Gastric Cancer* **2019**, *19*, 301–314. [CrossRef] [PubMed]
27. Avgeris, M.; Panoutsopoulou, K.; Papadimitriou, M.A.; Scorilas, A. Circulating exosomal miRNAs: Clinical significance in human cancers. *Expert Rev. Mol. Diagn.* **2019**, *19*, 979–995. [CrossRef]
28. Fang, Z.; Wang, X.; Wu, J.; Xiao, R.; Liu, J. High serum extracellular vesicle miR-10b expression predicts poor prognosis in patients with acute myeloid leukemia. *Cancer Biomark.* **2019**, *27*, 1–9. [CrossRef]
29. Jain, G.; Stuendl, A.; Rao, P.; Berulava, T.; Pena Centeno, T.; Kaurani, L.; Burkhardt, S.; Delalle, I.; Kornhuber, J.; Hull, M.; et al. A combined miRNA-piRNA signature to detect Alzheimer’s disease. *Transl. Psychiatry* **2019**, *9*, 250. [CrossRef] [PubMed]
30. Chen, C.; Luo, Y.; He, W.; Zhao, Y.; Kong, Y.; Liu, H.; Zhong, G.; Li, Y.; Li, J.; Huang, J.; et al. Exosomal long noncoding RNA LNMMAT2 promotes lymphatic metastasis in bladder cancer. *J. Clin. Investig.* **2019**, *130*, 404–421. [CrossRef] [PubMed]
31. Wang, Z.; Song, Y.; Han, X.; Qu, P.; Wang, W. Long noncoding RNA PTENP1 affects the recovery of spinal cord injury by regulating the expression of miR-19b and miR-21. *J. Cell. Physiol.* **2019**, *235*, 3634–3645. [CrossRef] [PubMed]
32. Azmi, A.S.; Bao, B.; Sarkar, F.H. Exosomes in cancer development, metastasis, and drug resistance: A comprehensive review. *Cancer Metastasis Rev.* **2013**, *32*, 623–642. [CrossRef] [PubMed]
33. Hu, L.; Wang, J.; Zhou, X.; Xiong, Z.; Zhao, J.; Yu, R.; Huang, F.; Zhang, H.; Chen, L. Exosomes derived from human adipose mesenchymal stem cells accelerates cutaneous wound healing via optimizing the characteristics of fibroblasts. *Sci. Rep.* **2016**, *6*, 32993. [CrossRef]
34. McDonald, M.K.; Tian, Y.; Qureshi, R.A.; Gormley, M.; Ertel, A.; Gao, R.; Aradillas Lopez, E.; Alexander, G.M.; Sacan, A.; Fortina, P.; et al. Functional significance of macrophage-derived exosomes in inflammation and pain. *Pain* **2014**, *155*, 1527–1539. [CrossRef]
35. Zhang, B.; Wang, M.; Gong, A.; Zhang, X.; Wu, X.; Zhu, Y.; Shi, H.; Wu, L.; Zhu, W.; Qian, H.; et al. HucMSC-Exosome Mediated-Wnt4 Signaling Is Required for Cutaneous Wound Healing. *Stem Cells* **2015**, *33*, 2158–2168. [CrossRef] [PubMed]
36. Haney, M.J.; Klyachko, N.L.; Zhao, Y.; Gupta, R.; Plotnikova, E.G.; He, Z.; Patel, T.; Piroyan, A.; Sokolsky, M.; Kabanov, A.V.; et al. Exosomes as drug delivery vehicles for Parkinson’s disease therapy. *J. Control. Release* **2015**, *207*, 18–30. [CrossRef] [PubMed]
37. Srinivas, L.; Deepthi, S.; Kgk, D.; Malla, R.R. Current Perspectives of Exosomes as Therapeutic Targets and Drug Delivery Vehicles for Pancreatic Cancer. *Crit. Rev. Oncog.* **2019**, *24*, 179–190. [CrossRef]
38. Zhang, D.; Lee, H.; Wang, X.; Rai, A.; Groot, M.; Jin, Y. Exosome-Mediated Small RNA Delivery: A Novel Therapeutic Approach for Inflammatory Lung Responses. *Mol. Ther.* **2018**, *26*, 2119–2130. [CrossRef]
39. Gonzalez, E.; Falcon-Perez, J.M. Cell-derived extracellular vesicles as a platform to identify low-invasive disease biomarkers. *Expert Rev. Mol. Diagn.* **2015**, *15*, 907–923. [CrossRef]
40. Trams, E.G.; Lauter, C.J.; Salem, N., Jr.; Heine, U. Exfoliation of membrane ecto-enzymes in the form of micro-vesicles. *Biochim. Biophys. Acta* **1981**, *645*, 63–70. [CrossRef]
41. Han, K.Y.; Tran, J.A.; Chang, J.H.; Azar, D.T.; Zieske, J.D. Potential role of corneal epithelial cell-derived exosomes in corneal wound healing and neovascularization. *Sci. Rep.* **2017**, *7*, 40548. [CrossRef] [PubMed]

42. Samaekia, R.; Rabiee, B.; Putra, I.; Shen, X.; Park, Y.J.; Hematti, P.; Eslani, M.; Djalilian, A.R. Effect of Human Corneal Mesenchymal Stromal Cell-derived Exosomes on Corneal Epithelial Wound Healing. *Investig. Ophthalmol. Vis. Sci.* **2018**, *59*, 5194–5200. [[CrossRef](#)] [[PubMed](#)]
43. Ueno, M.; Asada, K.; Toda, M.; Nagata, K.; Sotozono, C.; Kosaka, N.; Ochiya, T.; Kinoshita, S.; Hamuro, J. Concomitant Evaluation of a Panel of Exosome Proteins and MiRs for Qualification of Cultured Human Corneal Endothelial Cells. *Investig. Ophthalmol. Vis. Sci.* **2016**, *57*, 4393–4402. [[CrossRef](#)] [[PubMed](#)]
44. Zieske, J.D.; Hutcheon, A.E.K.; Guo, X. Extracellular Vesicles and Cell-Cell Communication in the Cornea. *Anat. Rec.* **2020**, *303*, 1727–1734. [[CrossRef](#)]
45. Leszczynska, A.; Kulkarni, M.; Ljubimov, A.V.; Saghizadeh, M. Exosomes from normal and diabetic human corneolimbal keratocytes differentially regulate migration, proliferation and marker expression of limbal epithelial cells. *Sci. Rep.* **2018**, *8*, 15173. [[CrossRef](#)]
46. Escandon, P.; Liu, A.; Nicholas, S.E.; Khan, A.; Riaz, K.M.; Karamichos, D. Unravelling Novel Roles of Salivary Exosomes in the Regulation of Human Corneal Stromal Cell Migration and Wound Healing. *Int. J. Mol. Sci.* **2022**, *23*, 4330. [[CrossRef](#)]
47. Ma, S.; Yin, J.; Hao, L.; Liu, X.; Shi, Q.; Diao, Y.; Yu, G.; Liu, L.; Chen, J.; Zhong, J. Exosomes from Human Umbilical Cord Mesenchymal Stem Cells Treat Corneal Injury via Autophagy Activation. *Front. Bioeng. Biotechnol.* **2022**, *10*, 879192. [[CrossRef](#)]
48. Wang, S.; Hou, Y.; Li, X.; Song, Z.; Sun, B.; Li, X.; Zhang, H. Comparison of exosomes derived from induced pluripotent stem cells and mesenchymal stem cells as therapeutic nanoparticles for treatment of corneal epithelial defects. *Aging* **2020**, *12*, 19546–19562. [[CrossRef](#)] [[PubMed](#)]
49. Edgar, J.R. Q&A: What are exosomes, exactly? *BMC Biol.* **2016**, *14*, 46.
50. Thery, C.; Witwer, K.W.; Aikawa, E.; Alcaraz, M.J.; Anderson, J.D.; Andriantsitohaina, R.; Antoniou, A.; Arab, T.; Archer, F.; Atkin-Smith, G.K.; et al. Minimal information for studies of extracellular vesicles 2018 (MISEV2018): A position statement of the International Society for Extracellular Vesicles and update of the MISEV2014 guidelines. *J. Extracell. Vesicles* **2018**, *7*, 1535750. [[CrossRef](#)]
51. Atkinson, M.A.; Appella, E.; Corigliano-Murphy, M.A.; Korn, E.D. Enzymatic activity and filament assembly of Acanthamoeba myosin II are regulated by adjacent domains at the end of the tail. *FEBS Lett.* **1988**, *234*, 435–438. [[CrossRef](#)]
52. Raposo, G.; Stoorvogel, W. Extracellular vesicles: Exosomes, microvesicles, and friends. *J. Cell Biol.* **2013**, *200*, 373–383. [[CrossRef](#)] [[PubMed](#)]
53. Lotvall, J.; Hill, A.F.; Hochberg, F.; Buzas, E.I.; Di Vizio, D.; Gardiner, C.; Gho, Y.S.; Kurochkin, I.V.; Mathivanan, S.; Quesenberry, P.; et al. Minimal experimental requirements for definition of extracellular vesicles and their functions: A position statement from the International Society for Extracellular Vesicles. *J. Extracell. Vesicles* **2014**, *3*, 26913. [[CrossRef](#)]
54. Consortium, E.-T.; Van Deun, J.; Mestdagh, P.; Agostinis, P.; Akay, O.; Anand, S.; Anckaert, J.; Martinez, Z.A.; Baetens, T.; Beghein, E.; et al. EV-TRACK: Transparent reporting and centralizing knowledge in extracellular vesicle research. *Nat. Methods* **2017**, *14*, 228–232. [[CrossRef](#)] [[PubMed](#)]
55. Fernandes-Cunha, G.M.; Na, K.S.; Putra, I.; Lee, H.J.; Hull, S.; Cheng, Y.C.; Blanco, I.J.; Eslani, M.; Djalilian, A.R.; Myung, D. Corneal Wound Healing Effects of Mesenchymal Stem Cell Secretome Delivered Within a Viscoelastic Gel Carrier. *Stem Cells Transl. Med.* **2019**, *8*, 478–489. [[CrossRef](#)]
56. Mobaraki, M.; Abbasi, R.; Omidian Vandchali, S.; Ghaffari, M.; Moztarzadeh, F.; Mozafari, M. Corneal Repair and Regeneration: Current Concepts and Future Directions. *Front. Bioeng. Biotechnol.* **2019**, *7*, 135. [[CrossRef](#)]
57. Zhang, Y.; Wu, X.H.; Luo, C.L.; Zhang, J.M.; He, B.C.; Chen, G. Interleukin-12-anchored exosomes increase cytotoxicity of T lymphocytes by reversing the JAK/STAT pathway impaired by tumor-derived exosomes. *Int. J. Mol. Med.* **2010**, *25*, 695–700.
58. Feng, N.; Jia, Y.; Huang, X. Exosomes from adipose-derived stem cells alleviate neural injury caused by microglia activation via suppressing NF- $\kappa$ B and MAPK pathway. *J. Neuroimmunol.* **2019**, *334*, 576996. [[CrossRef](#)]
59. Zhang, W.; Jiang, H.; Kong, Y. Exosomes derived from platelet-rich plasma activate YAP and promote the fibrogenic activity of Muller cells via the PI3K/Akt pathway. *Exp. Eye Res.* **2020**, *193*, 107973. [[CrossRef](#)]
60. Gurunathan, S.; Kang, M.H.; Jeyaraj, M.; Qasim, M.; Kim, J.H. Review of the Isolation, Characterization, Biological Function, and Multifarious Therapeutic Approaches of Exosomes. *Cells* **2019**, *8*, 307. [[CrossRef](#)]
61. Johnsen, K.B.; Gudbergsson, J.M.; Skov, M.N.; Pilgaard, L.; Moos, T.; Duroux, M. A comprehensive overview of exosomes as drug delivery vehicles—Endogenous nanocarriers for targeted cancer therapy. *Biochim. Biophys. Acta* **2014**, *1846*, 75–87. [[CrossRef](#)] [[PubMed](#)]
62. Lamichhane, T.N.; Raiker, R.S.; Jay, S.M. Exogenous DNA Loading into Extracellular Vesicles via Electroporation is Size-Dependent and Enables Limited Gene Delivery. *Mol. Pharm.* **2015**, *12*, 3650–3657. [[CrossRef](#)] [[PubMed](#)]
63. Meehan, K.; Vella, L.J. The contribution of tumour-derived exosomes to the hallmarks of cancer. *Crit. Rev. Clin. Lab. Sci.* **2016**, *53*, 121–131. [[CrossRef](#)]
64. Shen, T.; Zheng, Q.Q.; Shen, J.; Li, Q.S.; Song, X.H.; Luo, H.B.; Hong, C.Y.; Yao, K. Effects of Adipose-derived Mesenchymal Stem Cell Exosomes on Corneal Stromal Fibroblast Viability and Extracellular Matrix Synthesis. *Chin. Med. J.* **2018**, *131*, 704–712. [[CrossRef](#)] [[PubMed](#)]
65. Wahlgren, J.; Statello, L.; Skogberg, G.; Telemo, E.; Valadi, H. Delivery of Small Interfering RNAs to Cells via Exosomes. *Methods Mol. Biol.* **2016**, *1364*, 105–125. [[PubMed](#)]

66. Simpson, R.J.; Jensen, S.S.; Lim, J.W. Proteomic profiling of exosomes: Current perspectives. *Proteomics* **2008**, *8*, 4083–4099. [[CrossRef](#)]
67. Rani, S.; Ryan, A.E.; Griffin, M.D.; Ritter, T. Mesenchymal Stem Cell-derived Extracellular Vesicles: Toward Cell-free Therapeutic Applications. *Mol. Ther.* **2015**, *23*, 812–823. [[CrossRef](#)]
68. Guo, S.C.; Tao, S.C.; Yin, W.J.; Qi, X.; Yuan, T.; Zhang, C.Q. Exosomes derived from platelet-rich plasma promote the re-epithelialization of chronic cutaneous wounds via activation of YAP in a diabetic rat model. *Theranostics* **2017**, *7*, 81–96. [[CrossRef](#)]
69. Hu, Y.; Rao, S.S.; Wang, Z.X.; Cao, J.; Tan, Y.J.; Luo, J.; Li, H.M.; Zhang, W.S.; Chen, C.Y.; Xie, H. Exosomes from human umbilical cord blood accelerate cutaneous wound healing through miR-21-3p-mediated promotion of angiogenesis and fibroblast function. *Theranostics* **2018**, *8*, 169–184. [[CrossRef](#)]
70. Shi, H.; Xu, X.; Zhang, B.; Xu, J.; Pan, Z.; Gong, A.; Zhang, X.; Li, R.; Sun, Y.; Yan, Y.; et al. 3,3'-Diindolylmethane stimulates exosomal Wnt11 autocrine signaling in human umbilical cord mesenchymal stem cells to enhance wound healing. *Theranostics* **2017**, *7*, 1674–1688. [[CrossRef](#)]
71. McKay, T.B.; Hutcheon, A.E.K.; Zieske, J.D.; Ciolino, J.B. Extracellular Vesicles Secreted by Corneal Epithelial Cells Promote Myofibroblast Differentiation. *Cells* **2020**, *9*, 1080. [[CrossRef](#)] [[PubMed](#)]
72. Rashid, M.H.; Borin, T.F.; Ara, R.; Angara, K.; Cai, J.; Achyut, B.R.; Liu, Y.; Arbab, A.S. Differential in vivo biodistribution of (131)I-labeled exosomes from diverse cellular origins and its implication for theranostic application. *Nanomedicine* **2019**, *21*, 102072. [[CrossRef](#)]
73. Oh, M.; Lee, J.; Kim, Y.J.; Rhee, W.J.; Park, J.H. Exosomes Derived from Human Induced Pluripotent Stem Cells Ameliorate the Aging of Skin Fibroblasts. *Int. J. Mol. Sci.* **2018**, *19*, 1715. [[CrossRef](#)] [[PubMed](#)]
74. Xiong, J.; Liu, Z.; Wu, M.; Sun, M.; Xia, Y.; Wang, Y. Comparison of Proangiogenic Effects of Adipose-Derived Stem Cells and Foreskin Fibroblast Exosomes on Artificial Dermis Prefabricated Flaps. *Stem Cells Int.* **2020**, *2020*, 5293850. [[CrossRef](#)] [[PubMed](#)]
75. Thery, C.; Zitvogel, L.; Amigorena, S. Exosomes: Composition, biogenesis and function. *Nat. Rev. Immunol.* **2002**, *2*, 569–579. [[CrossRef](#)] [[PubMed](#)]
76. Garcia-Martin, R.; Brando, B.B.; Thomou, T.; Altindis, E.; Kahn, C.R. Tissue differences in the exosomal/small extracellular vesicle proteome and their potential as indicators of altered tissue metabolism. *Cell Rep.* **2022**, *38*, 110277. [[CrossRef](#)] [[PubMed](#)]
77. Andreu, Z.; Yanez-Mo, M. Tetraspanins in extracellular vesicle formation and function. *Front. Immunol.* **2014**, *5*, 442. [[CrossRef](#)] [[PubMed](#)]
78. Liao, Z.; Zhou, X.; Li, S.; Jiang, W.; Li, T.; Wang, N.; Xiao, N. Activation of the AKT/GSK-3beta/beta-catenin pathway via photobiomodulation therapy promotes neural stem cell proliferation in neonatal rat models of hypoxic-ischemic brain damage. *Ann. Transl. Med.* **2022**, *10*, 55. [[CrossRef](#)]
79. Meng, J.; Liu, H.L.; Ma, D.; Wang, H.Y.; Peng, Y.; Wang, H.L. Upregulation of aurora kinase A promotes vascular smooth muscle cell proliferation and migration by activating the GSK-3beta/beta-catenin pathway in aortic-dissecting aneurysms. *Life Sci.* **2020**, *262*, 118491. [[CrossRef](#)]
80. Sun, J.; Yan, P.; Chen, Y.; Chen, Y.; Yang, J.; Xu, G.; Mao, H.; Qiu, Y. MicroRNA-26b inhibits cell proliferation and cytokine secretion in human RASF cells via the Wnt/GSK-3beta/beta-catenin pathway. *Diagn. Pathol.* **2015**, *10*, 72. [[CrossRef](#)]
81. Yun, S.H.; Park, J.I. PGC-1alpha Regulates Cell Proliferation and Invasion via AKT/GSK-3beta/beta-catenin Pathway in Human Colorectal Cancer SW620 and SW480 Cells. *Anticancer Res.* **2020**, *40*, 653–664. [[CrossRef](#)] [[PubMed](#)]
82. Zhu, Z.; Yin, J.; Guan, J.; Hu, B.; Niu, X.; Jin, D.; Wang, Y.; Zhang, C. Lithium stimulates human bone marrow derived mesenchymal stem cell proliferation through GSK-3beta-dependent beta-catenin/Wnt pathway activation. *FEBS J.* **2014**, *281*, 5371–5389. [[CrossRef](#)] [[PubMed](#)]
83. Jiang, J.; Cheng, Y.; Dai, S.; Zou, B.; Guo, X. Suppression of rhomboid domain-containing 1 produces anticancer effects in pancreatic adenocarcinoma through affection of the AKT/GSK-3beta/beta-catenin pathway. *Environ. Toxicol.* **2022**, *37*, 1944–1956. [[CrossRef](#)] [[PubMed](#)]
84. Pan, J.; Fan, Z.; Wang, Z.; Dai, Q.; Xiang, Z.; Yuan, F.; Yan, M.; Zhu, Z.; Liu, B.; Li, C. CD36 mediates palmitate acid-induced metastasis of gastric cancer via AKT/GSK-3beta/beta-catenin pathway. *J. Exp. Clin. Cancer Res.* **2019**, *38*, 52. [[CrossRef](#)]
85. Tan, D.; Zhang, Y. Silencing of Nudix type 5 represses proliferation and invasion and enhances chemosensitivity of gastric carcinoma cells by affecting the AKT/GSK-3beta/beta-catenin pathway. *Toxicol. Appl. Pharmacol.* **2022**, *441*, 115968. [[CrossRef](#)]
86. Yang, L.; Tan, W.; Wei, Y.; Xie, Z.; Li, W.; Ma, X.; Wang, Q.; Li, H.; Zhang, Z.; Shang, C.; et al. CircLIFR suppresses hepatocellular carcinoma progression by sponging miR-624-5p and inactivating the GSK-3beta/beta-catenin signaling pathway. *Cell Death Dis.* **2022**, *13*, 464. [[CrossRef](#)]
87. Zhang, P.; Tian, Q.; Gao, H.; Zhao, A.; Shao, Y.; Yang, J. Inhibition of MAC30 exerts antitumor effects in nasopharyngeal carcinoma via affecting the Akt/GSK-3beta/beta-catenin pathway. *J. Biochem. Mol. Toxicol.* **2022**, *36*, e23061. [[CrossRef](#)] [[PubMed](#)]
88. Liu, C.; Li, Y.; Semenov, M.; Han, C.; Baeg, G.H.; Tan, Y.; Zhang, Z.; Lin, X.; He, X. Control of beta-catenin phosphorylation/degradation by a dual-kinase mechanism. *Cell* **2002**, *108*, 837–847. [[CrossRef](#)]
89. Salahshor, S.; Woodgett, J.R. The links between axin and carcinogenesis. *J. Clin. Pathol.* **2005**, *58*, 225–236. [[CrossRef](#)] [[PubMed](#)]
90. Yang, J.; Caldwell, R.B.; Behzadian, M.A. Blockade of VEGF-induced GSK/beta-catenin signaling, uPAR expression and increased permeability by dominant negative p38alpha. *Exp. Eye Res.* **2012**, *100*, 101–108. [[CrossRef](#)]

91. Yong, J.; von Bremen, J.; Ruiz-Heiland, G.; Ruf, S. Adiponectin as Well as Compressive Forces Regulate in vitro beta-Catenin Expression on Cementoblasts via Mitogen-Activated Protein Kinase Signaling Activation. *Front. Cell Dev. Biol.* **2021**, *9*, 645005. [[CrossRef](#)]
92. Bikkavilli, R.K.; Feigin, M.E.; Malbon, C.C. p38 mitogen-activated protein kinase regulates canonical Wnt-beta-catenin signaling by inactivation of GSK3beta. *J. Cell Sci.* **2008**, *121 Pt 21*, 3598–3607. [[CrossRef](#)]
93. Li, S.; Gallup, M.; Chen, Y.T.; McNamara, N.A. Molecular mechanism of proinflammatory cytokine-mediated squamous metaplasia in human corneal epithelial cells. *Investig. Ophthalmol. Vis. Sci.* **2010**, *51*, 2466–2475. [[CrossRef](#)] [[PubMed](#)]
94. Zhang, D.; Guo, M.; Zhang, W.; Lu, X.Y. Adiponectin stimulates proliferation of adult hippocampal neural stem/progenitor cells through activation of p38 mitogen-activated protein kinase (p38MAPK)/glycogen synthase kinase 3beta (GSK-3beta)/beta-catenin signaling cascade. *J. Biol. Chem.* **2011**, *286*, 44913–44920. [[CrossRef](#)] [[PubMed](#)]
95. Peake, P.W.; Kriketos, A.D.; Campbell, L.V.; Shen, Y.; Charlesworth, J.A. The metabolism of isoforms of human adiponectin: Studies in human subjects and in experimental animals. *Eur. J. Endocrinol.* **2005**, *153*, 409–417. [[CrossRef](#)] [[PubMed](#)]
96. Shapiro, L.; Scherer, P.E. The crystal structure of a complement-1q family protein suggests an evolutionary link to tumor necrosis factor. *Curr. Biol.* **1998**, *8*, 335–338. [[CrossRef](#)]
97. Shikama, Y.; Kurosawa, M.; Furukawa, M.; Ishimaru, N.; Matsushita, K. Involvement of adiponectin in age-related increases in tear production in mice. *Aging* **2019**, *11*, 8329–8346. [[CrossRef](#)]
98. Li, Y.; Jin, R.; Li, L.; Hsu, H.H.; You, I.C.; Yoon, H.J.; Yoon, K.C. Therapeutic Effect of Topical Adiponectin-Derived Short Peptides Compared with Globular Adiponectin in Experimental Dry Eye and Alkali Burn. *J. Ocul. Pharmacol. Ther.* **2020**, *36*, 88–96. [[CrossRef](#)]
99. Baradaran-Rafii, A.; Ashnagar, A.; Heidari Keshel, S.; Jabbehdari, S.; Baradaran-Rafii, G. Regression of corneal neovascularization: Adiponectin versus bevacizumab eye drops. *Eur. J. Ophthalmol.* **2021**, *31*, 78–82. [[CrossRef](#)] [[PubMed](#)]
100. Li, Z.; Cui, L.; Yang, J.M.; Lee, H.S.; Choi, J.S.; Woo, J.M.; Lim, S.K.; Yoon, K.C. The Wound Healing Effects of Adiponectin Eye Drops after Corneal Alkali Burn. *Curr. Eye Res.* **2016**, *41*, 1424–1432. [[CrossRef](#)] [[PubMed](#)]
101. Obata, Y.; Kita, S.; Koyama, Y.; Fukuda, S.; Takeda, H.; Takahashi, M.; Fujishima, Y.; Nagao, H.; Masuda, S.; Tanaka, Y.; et al. Adiponectin/T-cadherin system enhances exosome biogenesis and decreases cellular ceramides by exosomal release. *JCI Insight* **2018**, *3*, e99680. [[CrossRef](#)] [[PubMed](#)]
102. Acunzo, J.; Andrieu, C.; Baylot, V.; So, A.; Rocchi, P. Hsp27 as a therapeutic target in cancers. *Curr. Drug Targets* **2014**, *15*, 423–431. [[CrossRef](#)]
103. Jego, G.; Hazoume, A.; Seigneuric, R.; Garrido, C. Targeting heat shock proteins in cancer. *Cancer Lett.* **2013**, *332*, 275–285. [[CrossRef](#)]
104. Han, L.; Jiang, Y.; Han, D.; Tan, W. Hsp27 regulates epithelial mesenchymal transition, metastasis and proliferation in colorectal carcinoma. *Oncol. Lett.* **2018**, *16*, 5309–5316. [[CrossRef](#)] [[PubMed](#)]
105. Shen, C.; Liu, W.; Zhang, S.; Pu, L.; Deng, B.; Zeng, Q.; Chen, Z.; Wang, X. Downregulation of miR-541 induced by heat stress contributes to malignant transformation of human bronchial epithelial cells via HSP27. *Environ. Res.* **2020**, *184*, 108954. [[CrossRef](#)]
106. Sims, J.T.; Ganguly, S.S.; Bennett, H.; Friend, J.W.; Tepe, J.; Plattner, R. Imatinib reverses doxorubicin resistance by affecting activation of STAT3-dependent NF-kappaB and HSP27/p38/AKT pathways and by inhibiting ABCB1. *PLoS ONE* **2013**, *8*, e55509. [[CrossRef](#)] [[PubMed](#)]
107. Joyce, N.C. Proliferative capacity of the corneal endothelium. *Prog. Retin. Eye Res.* **2003**, *22*, 359–389. [[CrossRef](#)]
108. Imanishi, J.; Kamiyama, K.; Iguchi, I.; Kita, M.; Sotozono, C.; Kinoshita, S. Growth factors: Importance in wound healing and maintenance of transparency of the cornea. *Prog. Retin. Eye Res.* **2000**, *19*, 113–129. [[CrossRef](#)]
109. Li, D.Q.; Tseng, S.C. Three patterns of cytokine expression potentially involved in epithelial-fibroblast interactions of human ocular surface. *J. Cell. Physiol.* **1995**, *163*, 61–79. [[CrossRef](#)]
110. Wilson, S.E.; Chen, L.; Mohan, R.R.; Liang, Q.; Liu, J. Expression of HGF, KGF, EGF and receptor messenger RNAs following corneal epithelial wounding. *Exp. Eye Res.* **1999**, *68*, 377–397. [[CrossRef](#)]
111. Stepp, M.A. Corneal integrins and their functions. *Exp. Eye Res.* **2006**, *83*, 3–15. [[CrossRef](#)]
112. McKay, T.B.; Yeung, V.; Hutcheon, A.E.K.; Guo, X.; Zieske, J.D.; Ciolino, J.B. Extracellular Vesicles in the Cornea: Insights from Other Tissues. *Anal. Cell. Pathol.* **2021**, *2021*, 9983900. [[CrossRef](#)]
113. Theriault, M.; Gendron, S.P.; Brunette, I.; Rochette, P.J.; Proulx, S. Function-Related Protein Expression in Fuchs Endothelial Corneal Dystrophy Cells and Tissue Models. *Am. J. Pathol.* **2018**, *188*, 1703–1712. [[CrossRef](#)]
114. Peh, G.S.; Chng, Z.; Ang, H.P.; Cheng, T.Y.; Adnan, K.; Seah, X.Y.; George, B.L.; Toh, K.P.; Tan, D.T.; Yam, G.H.; et al. Propagation of human corneal endothelial cells: A novel dual media approach. *Cell Transplant.* **2015**, *24*, 287–304. [[CrossRef](#)]
115. Bisson, F.; Rochefort, E.; Lavoie, A.; Larouche, D.; Zaniolo, K.; Simard-Bisson, C.; Damour, O.; Auger, F.A.; Guerin, S.L.; Germain, L. Irradiated human dermal fibroblasts are as efficient as mouse fibroblasts as a feeder layer to improve human epidermal cell culture lifespan. *Int. J. Mol. Sci.* **2013**, *14*, 4684–4704. [[CrossRef](#)] [[PubMed](#)]
116. Thery, C.; Amigorena, S.; Raposo, G.; Clayton, A. Isolation and characterization of exosomes from cell culture supernatants and biological fluids. *Curr. Protoc. Cell Biol.* **2006**, *3*, 3–22. [[CrossRef](#)] [[PubMed](#)]
117. Le-Bel, G.; Cortez Ghio, S.; Larouche, D.; Germain, L.; Guerin, S.L. Qualitatively Monitoring Binding and Expression of the Transcription Factors Sp1 and NFI as a Useful Tool to Evaluate the Quality of Primary Cultured Epithelial Stem Cells in Tissue Reconstruction. *Methods Mol. Biol.* **2019**, *1879*, 43–73.

118. Couture, C.; Zaniolo, K.; Carrier, P.; Lake, J.; Patenaude, J.; Germain, L.; Guerin, S.L. The tissue-engineered human cornea as a model to study expression of matrix metalloproteinases during corneal wound healing. *Biomaterials* **2016**, *78*, 86–101. [[CrossRef](#)] [[PubMed](#)]
119. Desjardins, P.; Couture, C.; Germain, L.; Guerin, S.L. Contribution of the WNK1 kinase to corneal wound healing using the tissue-engineered human cornea as an in vitro model. *J. Tissue Eng. Regen. Med.* **2019**, *13*, 1595–1608. [[CrossRef](#)] [[PubMed](#)]
120. Xia, J.; Gill, E.E.; Hancock, R.E. NetworkAnalyst for statistical, visual and network-based meta-analysis of gene expression data. *Nat. Protoc.* **2015**, *10*, 823–844. [[CrossRef](#)]
121. Kramer, A.; Green, J.; Pollard, J., Jr.; Tugendreich, S. Causal analysis approaches in Ingenuity Pathway Analysis. *Bioinformatics* **2014**, *30*, 523–530. [[CrossRef](#)] [[PubMed](#)]